SAPIENZA
Università di Roma
Facoltà di Farmacia e Medicina

Ph.D. in
MORPHOGENESIS AND TISSUE ENGINEERING

XXXVII Cycle
(A.A. 2023/2024)

Unveiling the spermatogonial stem cell niche in primates: a histological approach

Ph.D. Student
Martina Palazzoli

Tutor
Prof.ssa Elena Vicini

Coordinator
Prof. Antonio Musarò

CONFIDENTIALITY NOTICE

Reviewers and PhD committee members are obliged to keep the files confidential and to delete all records after completing the review process.

Il ricevimento degli elaborati scientifici, per l'ottenimento del titolo di Dottore di Ricerca, in qualità di Membro del Collegio dei Docenti del Dottorato in Morfogenesi ed Ingegneria Tissutale richiede di osservare le seguenti normative:

i. considerare le Informazioni confidenziali e riservate come strettamente private e ad adottare tutte le ragionevoli misure finalizzate a mantenerle tali;

ii. utilizzare le Informazioni confidenziali e riservate unicamente allo scopo per le quali sono state fornite o rese note, impegnandosi a non divulgarle a soggetti terzi le informazioni contenute negli elaborati ricevuti;

iii. a garantire la massima riservatezza, anche in osservanza alla vigente normativa in materia di marchi, di copyright e di brevetti per invenzioni industriali e in base alla normativa sulla privacy, ai sensi del D.Lgs. 196/2003, riguardo il know-how e tutte le informazioni acquisite, che non potranno in alcun modo, in alcun caso e per alcuna ragione essere utilizzate a proprio o altrui profitto e/o essere divulgate e/o riprodotte o comunque rese note a soggetti terzi.

INDEX

1. SUMMARY..... 5
2. INTRODUCTION 7
2.1 Testis histology 7
2.2 Spermatogenesis..... 9
2.2.1 The seminiferous epithelium cycle..... 11
2.2.2 Regulation of spermatogenesis 14
2.3 The spermatogonial compartment 15
2.3.1 Molecular phenotype of spermatogonia 18
2.3.2 Trascriptome profile of spermatogonial subsets..... 19
2.3.3 Localization of spermatogonial stem cell niche..... 24
2.3.4 Kinetic of primate spermatogonial compartment... 26
3. AIMS 30
4. RESULTS..... 32
4.1 Characterization of putative cell-cell interactions occurring between somatic cells and spermatogonial stem cells……32
4.1.1 Protein expression of putative Ligand- Rceptor pairs in human and monkey testis sections 32
4.1.2 Histological distribution of the specific cell types expressing BMP4-BMPR1B Ligand-Rceptor pair. 38
4.1.3 Characterization of the specific cell types expressing BMPR1B in monkeys whole mounted tubules..... 40
4.1.4 Characterization of the specific cell types expressing BMPR1B in human whole mounted tubules..... 43
4.1.5 The kinetics of BMPR1B spermatogonia in monkey 46
4.2 Evaluation of the histological distribution of different spermatogonia subpopulation during the seminiferous epithelium cycle. 49

4.2.1 The topographical localization of undifferentiated spermatogonial subpopulations within the testis parenchyma 49
4.2.2. The topographical localization of differentiating spermatogonial subpopulations within the testis parenchyma ……53
5. DISCUSSION 57
6. MATERIALS AND METHODS.....64
6.1 Testicular biopsies 64
6.2 Immunofluorescence on FFPE 65
6.3 Immunohistochemistry on FFPE 65
6.4 Whole-mount immunofluorescence.....67
6.5 Determination of the stages of the cycle of the seminiferous epithelium. 68
6.6 Imaging and quantification 68
6.7 Determining the position of spermatogonia in testicular parenchyma.....69
6.8 Statistical analysis.....70
7. BIBLYOGRAPHY 71
8. LIST OF PUBLICATIONS 86
9. ATTACHMENT.....88
10. ANSWERS TO THE REVIEWERS.....93

1. SUMMARY

The maintenance of seminiferous epithelium function depends on the intricate molecular and cellular interactions between spermatogonial stem cells (SSCs) and their cognate niche. To sustain the continuous production of sperm, a delicate balance must prevail among the various niche factors that control the fate decisions of SSCs by promoting either self-renewal or spermatogenic commitment of undifferentiated spermatogonia (undiff-SPG). Despite its critical importance, our understanding of SSC homeostasis remains limited, particularly regarding the spatial distribution of SSCs within the testicular microenvironment. Here, we aim to characterize the SSC niche and its regulation in primates by identifying novel putative cell-cell interactions between somatic cells and SSCs, and by evaluating the histological distribution of different spermatogonia subpopulations during the seminiferous epithelium cycle. To this end, we analyzed the expression of established markers as well as novel markers identified by Single-cell RNA sequencing (sc-RNAseq) in the spermatogonial compartment of humans and *Macaca fascicularis*. Specifically, we sought to analyze the topological distribution of positive cells within the tubules (i.e., tubule-tubule or tubule-interstitium contact regions) during different stages of the seminiferous epithelium cycle. To validate protein expression, intact seminiferous tubules and sections from *Macaca fascicularis* and human testis biopsies were stained by immunofluorescence and analyzed by confocal microscopy. To analyze the topological position of spermatogonia in the seminiferous tubules, immunohistochemistry was performed on *Macaca fascicularis* Bouin-fixed samples, which were analyzed by light microscopy. Strauss's linear selectivity index (Linear Index, Li) was employed to analyze region selection by the various spermatogonia subpopulations in the basal compartment of seminiferous tubules in monkeys.

The analysis of protein expression of the published L-R (Ligand-Receptor) pairs we selected (BMP4-BMPR1B and WNT5A-RYK) revealed that only the BMP4-BMPR1B pair showed a positive correlation between RNA and protein expression in both human and monkey testis. Nevertheless, protein analysis showed that BMPR1B has a broader expression pattern compared to scRNAseq data, as it is expressed by all undiff-SPG and in a small percentage of differentiating spermatogonia (diff-SPG). Interestingly, BMP4 was found to be expressed in the interstitial Leydig cells in both human and monkey testis, suggesting that the BMP4-BMPR1B pair represents a functional putative somatic-to-germ cell interaction. Remarkably, our examination of the SPG subsets' relative positioning along the basal membrane in relation to interstitial tissue revealed significant distinctions. While PIWIL4^{+} undiff-SPG exhibited random distribution along the basal compartment across all the stages of the seminiferous epithelium cycle, GFRA1^{+} and NANOS3^{+} undiff-SPG, as well as c-KIT+ diff-SPG, displayed stage-dependent localization patterns. During the first half of the seminiferous epithelium cycle, GFRA1^{+} undiff-SPG occupied tubular regions adjacent to the interstitium, whereas in the second half they preferentially resided in tubule-tubule contact regions. NANOS3^{+} undiff-SPG, on the other hand, preferentially resided in regions facing the interstitium only at stages VI-VII, while from stage X to stage I, they predominantly inhabited tubule-tubule contact regions. Finally, c-KIT^{+} diff-SPG also preferentially resided in regions facing the interstitium, but only at stage VI-VII. The spatial organization of different SPG subsets appears to be coordinated with the stages of the seminiferous epithelium cycle, suggesting dynamic regulation of SSC behavior throughout sperm production. Our study contributes to the growing body of literature aimed at deciphering the complexities of SSC biology and the regulation of spermatogenesis in mammalian species, with implications for understanding male fertility.

2. INTRODUCTION

2.1 Testis histology

The testis is the male reproductive organ, responsible for two primary functions: the production of sex hormones and sperm. These functions are essential for maintaining male fertility. The testis is encased in a dense fibrous capsule called the tunica albuginea, which extends inward, forming the testicular parenchyma, and also defines the rete testis and the mediastinum. Functionally, the testis parenchyma is organized into two compartments: the interstitium and the seminiferous tubules. The interstitial compartment of the testis contains lymphatic and blood vessels, nerve fibers, Leydig cells, and other cell types. Leydig cells are somatic cells organized in clusters that produce steroids, such as testosterone and dehydroepiandrosterone (DHEA). These cells are easily recognizable due to their large round nucleus with a prominent nucleolus (Fig. 1A).

The seminiferous tubules form the tubular component of the testis and are subdivided into different layers: from the outer wall to the center, they consist of the tunica propria, seminiferous epithelium, and tubular lumen. The tunica propria contains peritubular smooth muscle-like myoid cells, along with collagen and laminin fibers. The seminiferous epithelium is a highly organized lining, made up of germ cells at various stages of differentiation and Sertoli cells, the only somatic cell type in the seminiferous epithelium, which play a vital role in initiating and maintaining spermatogenesis.

No blood vessels, nerves, or other cell types are found within the seminiferous epithelium. Germ cells, which are the precursors to mature gametes, are classified as spermatogonial stem cells, spermatogonia, spermatocytes, spermatids, and testicular spermatozoa (Fietz and Bergmann, 2017).

Spermatogenesis is the process of cellular differentiation in which spermatogonial stem cells develop into spermatozoa. This highly regulated process is sustained by Sertoli cells, whose cytoplasm surrounds and supports germ cells at each stage of differentiation. Sertoli cells provide hormones and growth factors, such as AMH and GDNF, necessary for gamete maturation, while their unique structure helps anchor germ cells and facilitate their movement through the seminiferous epithelium. These cells are connected by tight junctions that form the blood-testis barrier (BTB), dividing the seminiferous epithelium into a basal compartment (containing spermatogonia and preleptotene and leptotene primary spermatocytes) and an adluminal compartment (containing spermatids and spermatozoa), which benefit from immune privileges (Fig. 1B).

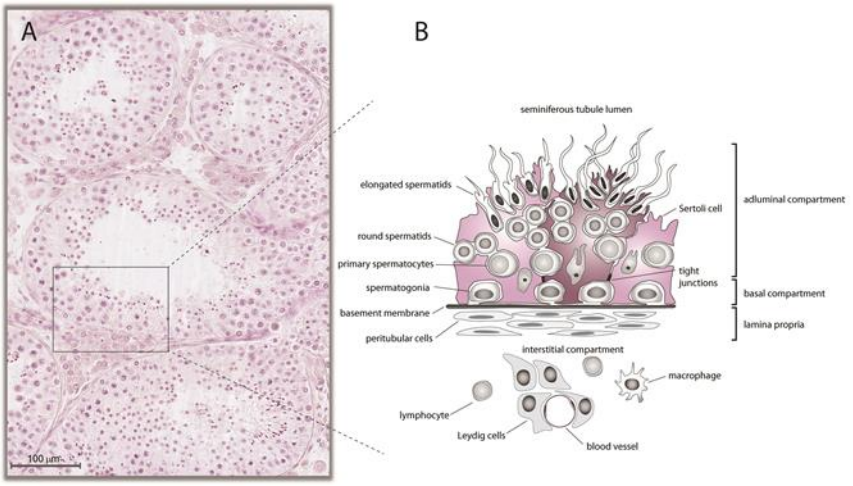

Figure 1: *Morphology of a human seminiferous tubule. A) Formalin-fixed, carmallume-stained testis section from 19-year-old man. B) Schematic representation of the human seminiferous tubule and the interstitial compartment (Capponi & Vicini, 2023).*

2.2 Spermatogenesis

In mammals, spermatogenesis is a continuous, cyclical process that can be divided into four main phases: the mitotic phase, the meiotic phase, spermiogenesis, and spermiation. The spermatogonia compartment comprise stem, undifferentiated and dfifferentiating cell types. During the mitotic phase, there is a large amplification of the spermatogonial compartment in which diploid SSCs undergo mitosis followed by incomplete cytokinesis, generating chains of spermatogonia and ultimately form spermatocytes connected by intercellular bridges. These spermatocytes enter the meiotic phase. Meiosis is a germ cell-specific process involving two consecutive divisions (meiosis I and II) but only one round of DNA replication, resulting in haploid germ cells. Meiosis I features a prolonged prophase I, subdivided into four stages: leptotene, zygotene, pachytene, and diplotene, each characterized by distinct nuclear morphologies. At the end of meiotic division, one diploid spermatocyte generates four haploid spermatids. These new spermatids undergo spermiogenesis, a significant morphological and functional transformation: the chromatin of the round spermatids starts to condensate, the nuclear shape changes, the excess cytoplasm is removed, and the acrosome and the sperm tail develop. All this process converts round haploid germ cells into highly polarized spermatozoa. At the end spermiation occurs and the spermatozoa are released into the lumen of the seminiferous tubules (Fig. 2) (Huckins and Oakberg, 1978).

Despite being a highly conserved process, spermatogenesis exhibits notable differences between primates and rodents, such as the composition of the spermatogonial compartment, the three-dimensional organization of the seminiferous tubules, the morphology of mature spermatozoa, the duration of the process, and daily sperm production.

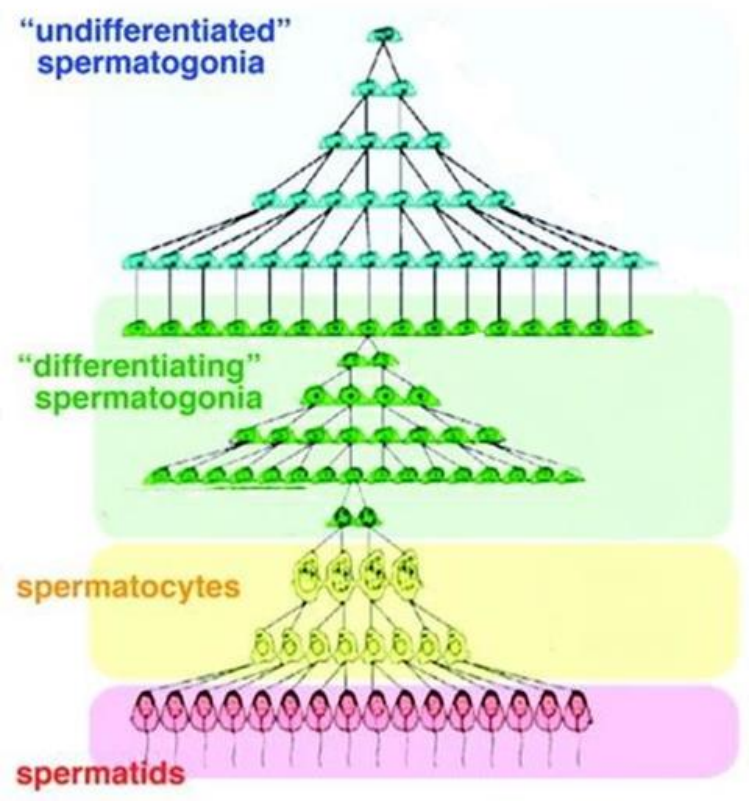

***Figure 2**: Scheme of spermatogenic process. The basal compartment is occupied by all the spermatogonia, including stem cells, while spermatocytes and spermatids are stratified to the lumen. Modified from (Yoshida, 2010)*

2.2.1 The seminiferous epithelium cycle

The continuous production of sperm cells through a highly regulated process occurs in cycles, referred to as the cycle of the seminiferous epithelium. Each cycle is characterized by specific stages during which distinct types of germ cells are present, progressing in a coordinated manner from undiff-SPG to mature spermatozoa.
The cycle of the seminiferous epithelium is a highly dynamic process that can be morphologically subdivided into a series of stages, each representing a unique combination of germ cells at various points in their development. These stages follow a strict temporal sequence and repeat cyclically. The exact number of stages and the timing of the cycle can vary across species. For example, in humans, the cycle lasts approximately 16 days, whereas in mice, it is much shorter, around 8.6 days (Hess and Renato de Franca, 2008). Despite these differences, the overall organization of the cycle ensures a continuous supply of sperm, as multiple generations of germ cells coexist within the seminiferous tubules at different stages of maturation.
Each phase of spermatogenesis is tightly regulated and varies by species. Consequently, the entire process of producing spermatozoa from diff-SPG takes approximately 35 days in mice and 74 days in humans (Heller and Clermont, 1963; Oakberg, 1956). As germ cells mature, they migrate from the basal compartment to the lumen, where they are released as mature spermatozoa. Meanwhile, new generations of diff-SPG are continuously produced even before the first generation reaches the lumen. As a result, multiple generations of germ cells coexist within different regions of the seminiferous epithelium. Each stage consistently features the same types of germ cells, allowing for stage identification based on the developmental progress of one generation of germ cells, typically through cytological or histological methods. Traditionally, stages have been characterized

by the morphology of the acrosome in spermatids, assessed using PAS staining in conventional paraffin-embedded testis sections. This method has been used across various mammals, often revealing 12 discernible stages, as observed in mice, monkeys, and humans (Fig. 3). However, in humans, PAS staining does not clearly define acrosome development. Therefore, stages are identified by combining the morphology of spermatid nuclei, the presence of other relevant germ cell types, and, more recently, ACR or Lectin PNA staining (IHC or IF) to detect acrosomal development (Capponi et al., 2023; Di Persio et al., 2021; Muciaccia et al., 2013).

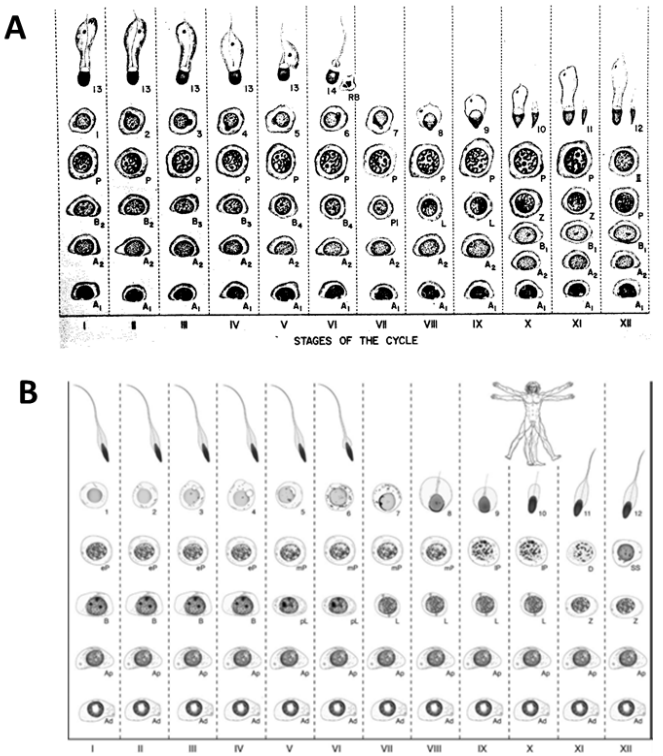

Figure 3: *Stages in the cycle of seminiferous epithelium in the monkey Cercopithecus aethiops (A) (Clermont 1969) and man (B) (Muciaccia et al., 2013).*

In most mammals, including rodents, the stages of spermatogenesis are well-defined, occupying specific regions of the seminiferous tubules. In contrast, in humans, the organization is less distinct. Instead of occupying a complete cross-section of the tubule, the stages appear in small, patchy areas of the basement membrane, often resulting in the presence of multiple stages within a single cross-section. This makes identifying the stages more challenging but also highlights the unique organizational structure of human spermatogenesis (Fig. 4).

Despite these variations, the cycle of the seminiferous epithelium remains a critical aspect of sperm production across species, ensuring the continuous renewal and development of germ cells necessary for male fertility.

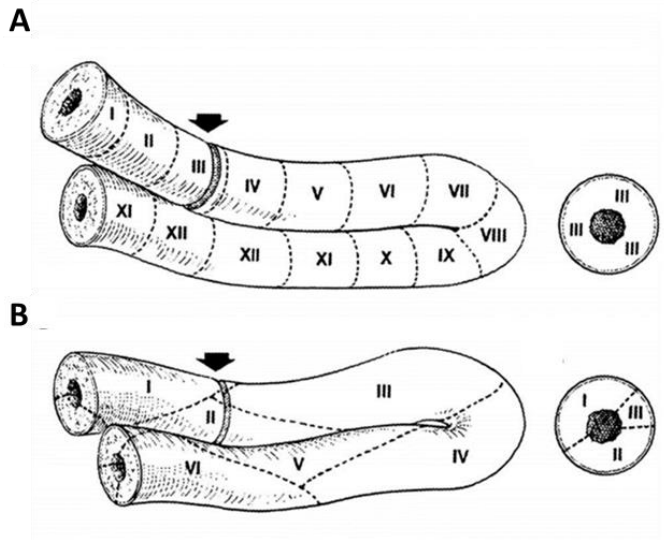

Figure 4: *Distribution of the stages of the seminiferous epithelium cycle in monkey (A) and in human (B). A) In Monkey, as in rodents, each stage occupies a long stretch of a tubule, showing a linear distribution, so that in a cross-section one stage can be found. B) Human stages present an helicoidal distribution and occupy a small portion of seminiferous tubules, within multiples stages in a cross-section (Schwarzer et al., 2003).*

2.2.2 Regulation of spermatogenesis

The regulation of spermatogenesis involves a fine-tuned interplay of hormones, local factors, and cell-to-cell signaling, ensuring the proper development and maturation of sperm cells.
The primary regulators, the endocrine ones, are the hypothalamic-pituitary-gonadal (HPG) axis and local factors within the testes. The process begins when the hypothalamus secretes gonadotropin-releasing hormone (GnRH), which stimulates the anterior pituitary gland to release luteinizing hormone (LH) and follicle-stimulating hormone (FSH). FSH signaling promotes the production of Inhibin B by Sertoli cells, which in turn provides negative feedback to regulate FSH levels (de Kretser et al., 2001). Conversely, LH stimulates Leydig cells to produce testosterone, which acts as negative feedback on the pituitary gland to inhibit LH production (Zirkin and Papadopoulos, 2018). In the absence of FSH and LH, only undifferentiated germ cells and Sertoli cells are found in the seminiferous tubules of the testis (Khanehzad et al., 2021).
Paracrine regulation is primarily mediated by retinoic acid (RA), which is produced by Sertoli cells and pachytene spermatocytes (Endo et al., 2017). RA plays several key roles: it promotes Sertoli cell maturation at puberty by inhibiting proliferation (Nicholls et al., 2013), facilitates spermatogonial differentiation (van Pelt and de Rooij, 1991), induces meiosis (Koubova et al., 2006), maintains blood-testis barrier (BTB) integrity (Morales and Cavicchia, 2002), supports spermiation (Vernet et al., 2008), and coordinates the adult spermatogenic cycle (Endo et al., 2015; Sugimoto et al., 2012). RA also enhances differentiation by downregulating GDNF expression in Sertoli cells (Saracino et al., 2020). In both rodents and primates, GDNF is primarily produced by Sertoli cells (Davidoff et al., 2001; Golden et al., 1999; Trupp et al., 1995). In humans, both pale and dark spermatogonia express the GDNF receptor GFRA1 (Grisanti et al., 2009), which is found in 54% of the spermatogonial compartment cells (Di Persio et al., 2017).

The function of GDNF in the human testis remains poorly understood, although it is hypothesized to have a role similar to that in rodents. GDNF positively regulates several genes crucial for spermatogonial self-renewal, including Bcl6b (B cell CLL/lymphoma 6 member B), Erm (Ets variant 5), and Lhx1 (LIM homeobox 1) (Oatley et al., 2007; Oatley and Brinster, 2008). Additionally, GDNF stimulates spermatogonia to express its receptor GFRA1 (Grasso et al., 2012) and the Fibroblast Growth Factor 2 receptor (FGFR2), enhancing the cells' responsiveness to GDNF, which in turn promotes SSC self-renewal (Hara et al., 2014; Nakamura et al., 2021). GDNF may also support spermatogonial self-renewal by inhibiting spermatogonial differentiation (Sharma and Braun, 2018). Other local signals, such as CSF-1 (Colony Stimulating Factor 1), produced by macrophages, contribute to the maintenance and proliferation of SSCs (DeFalco et al., 2015).

2.3 The spermatogonial compartment

In all mammals, SPG are categorized into SSCs, undiff-SPG, and diff-SPG. The distinction between undiff-SPG and diff-SPG is traditionally based on nuclear morphology and includes significant differences in marker expression, apoptotic regulation, and cell cycle dynamics (Boitani et al., 2016) (Fig. 5). However, between primates and rodents, there are some remarkable differences as the tridimensional organization of the seminiferous tubules, the daily sperm production (Amann, 2008), the morphology of the mature spermatozoa, the duration of the process (Heller and Clermont, 1964) and the composition of the spermatogonial compartment.

A

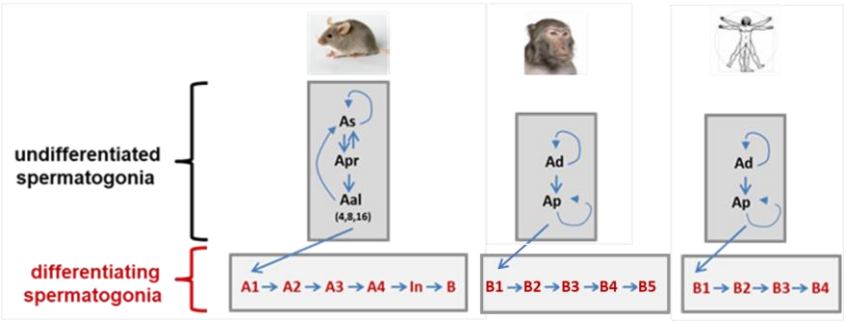

B

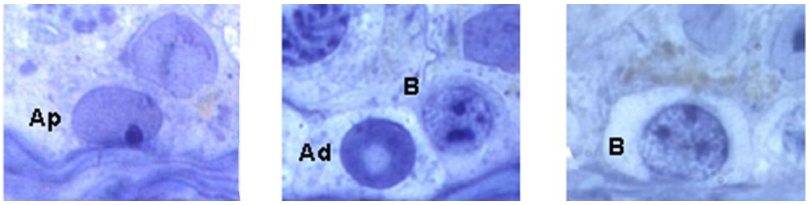

***Figure* 5:** *Spermatogonial compartment in mammals. A) Scheme of cell subtypes in mouse, monkey and man spermatogonial compartment. Modified from (Boitani et al., 2016).. B) Morphology of spermatogonia in the human seminiferous epithelium in semithin section of glutaraldeyde / OsO4-fixed tissue. Modified from (Muciaccia et al., 2013).*

In rodents, the spermatogonial population is typically categorized into two main groups: uundiff-SPG, which encompass SSCs, and diff-SPG. The undiff-SPG consists of A-single (As) spermatogonia, A-pair (Apr) spermatogonia pairs of daughter cells linked by an intracellular bridge due to incomplete cytokinesis and A-aligned (Aal) spermatogonia, which are chains of 4, 8, 16, or occasionally 32 cells connected by intercellular bridges. Undiff-SPG can mature into diff-SPG under the influence of retinoic acid. The diff-SPG includes A1, A2, A3, A4, Intermediate, and B spermatogonia (Fig. 5A).

Spermatogonia are arranged in a horizontal layer along the basement membrane of the seminiferous epithelium. During mitotic proliferation, they are organized as individual cells or

chains of various lengths, interconnected by cytoplasmic bridges due to incomplete cytokinesis (de Rooij and Russell, 2000). The B spermatogonia subsequently differentiates into primary spermatocytes, entering the meiotic phase of spermatogenesis.

In primates, including monkeys and humans, spermatogonia are divided into three morphologically distinct subpopulations: dark type A (Ad), pale type A (Ap), and type B. Ad and Ap spermatogonia are considered undifferentiated, whereas B spermatogonia are differentiated (Fig. 5A). Ad spermatogonia are distinguished by spherical or ovoid nuclei with densely stained, dust-like chromatin and a nucleolus at the nuclear periphery, while Ap spermatogonia have ovoid nuclei with lightly stained chromatin and a nucleolus at the nuclear periphery (Fig. 5B). Ad spermatogonia are typically quiescent, rarely incorporating S-phase markers (such as 3H-thymidine or BrdU) or expressing PCNA (a marker for proliferating cells) (Hermann et al., 2010). Ad and Ap spermatogonia are referred to as "reserve stem cells" and "active stem cells," respectively (Clermont, 1969). In non-human primates, quiescent Ad spermatogonia can be rapidly activated upon depletion of the Ap spermatogonia following cytotoxic treatment with ionizing radiation (van Alphen et al., 1988). Spermatogonia with an intermediate morphology between Ad and Ap are termed A-transition or A-unclassified in monkeys (Fouquet and Dadoune, 1986; Simorangkir et al., 2005). The precise relationship between Ad, Ap, and intermediate spermatogonia remains unclear, although it is generally believed that Ap spermatogonia give rise to B spermatogonia (Plant, 2010). The nuclei of B spermatogonia are spherical, characterized by finely granulated chromatin with some intensely stained chromatin clumps that may adhere to the nuclear envelope, which appears well-defined, with one or more centrally located nucleoli (Fig. 5B). Recent studies have identified three generations of B spermatogonia in humans (B1, B2, and B3) (Di Persio et al., 2017). In *Macaca mulatta*, B SPG are distinguished by variations in the granulation and density of heterochromatin staining, with B1 SPG being the least heterochromatic and B4

spermatogonia the most heterochromatic (Clermont et al., 1959). Recently, using KIT and PHH3 staining, the number of B SPG generations in *Macaca fascicularis* was re-assessed to five and not four as previously described (Capponi et al., 2023). The final generation of B SPG divides to form preleptotene spermatocytes, which then enter meiosis (Fig. 3).

2.3.1 Molecular phenotype of spermatogonia

In the last years, several laboratories have been involved in the study of the molecular signature of the different populations in the spermatogonial compartment. The main purpose was to identify molecular markers that could be used to isolate the spermatogonial stem cells and to develop a new approach to characterize the different spermatogonial subpopulations. Unfortunately, until now, it is not possible to identify a specific molecular marker of the SSC, both in the rodents and in the primates. The SSCs are still identified only by their ability to colonize and to produce spermatogenesis in testes of infertile mice, after transplantation (Brinster and Avarbock, 1994).

In mice, the proposed molecular signature for SSCs includes markers such as α6-integrin+, β1-integrin+, $THY1^+$, $CD9^+$, GFRA1+, with low Rho123 levels, and the absence of αV-integrin, KIT, MHC-I, ALDH, and CD45 (Oatley and Brinster, 2008). However, this signature remains a topic of debate. GFRA1 and NGN3 have emerged as critical markers in SSC specification, with $GFRA1^+$ cells (primarily As and Apr) being identified as the functional stem cells in steady state, while $NGN3^+$ cells (primarily Aal) are committed to differentiation. Remarkably, $NGN3^+$ cells retain the potential to act as stem cells following testicular damage (Nakagawa et al., 2021; Nakagawa et al., 2007; Nakagawa et al., 2010).

In primates, SPG-specific markers are diverse and do not always correlate with classical Ad/Ap nuclear morphology (Grisanti et al., 2009). Because of this observation, and because many A SPG cannot be unequivocally characterized as Ad or Ap, human undiff-SPG have been recently collectively defined as Ap-d SPG (Di Persio et al., 2017). In this classification, the Ad SPG and Ap SPG were included in the same population of UCHL-1 positive undiff-SPG (Tokunaga et al., 1999).

In rodents, undiff-SPG encompasses As, Apr, and some Aal spermatogonia, characterized by markers such as GFRA1+, PLZF+, and SALL4+ (Aponte et al., 2005). Markers conserved across rodents, non-human primates, and humans include GFRA1, UTF1, PLZF, SALL4, and LIN28 (Buaas et al., 2004; Costoya et al., 2004; Gassei and Orwig, 2013; Hermann et al., 2009; Meng et al., 2000; Ramaswamy et al., 2014; Zheng et al., 2009). Recently PIWIL4 has been indicated as another marker for undiff-SPG in primates (Capponi et al., 2023; Di Persio and Neuhaus, 2023; Sohni et al., 2019). Regarding the differentiating spermatogonial compartment, both in the mouse and in the primate, a universally accepted marker is KIT the Stem cell factor receptor. In the mouse, KIT starts to be expressed in the Aal during their differentiation to A1, induced by the retinoic acid and it remains expressed until the early stages of the meiotic prophase (Yoshinaga et al., 1991). KIT is a marker of differentiating spermatogonia also in non-human and human primates (monkey and man) (Hermann et al., 2009; Unni et al., 2009).

2.3.2 Trascriptome profile of spermatogonial subsets

Recent advancements have challenged the traditional, simplified view of spermatogonial compartment organization in primates, revealing a complex array of spermatogonial subsets with significant heterogeneity. The emergence of single-cell RNA

sequencing (scRNA-seq) technology has facilitated this paradigm shift, leading to the publication of several studies on human and monkey testes (Di Persio et al., 2021; Guo et al., 2018; Hermann et al., 2018; Shami et al., 2020; Sohni et al., 2019). These studies, alongside comparative research in mice and primates, have provided crucial insights into the SSC niche a specialized microenvironment that regulates SSC quiescence, self-renewal, survival, and differentiation (Shami et al., 2020).

Transcriptome analyses of isolated cells from primate testes have enabled the identification of major cell types, including germ cells (spermatogonia, spermatocytes, and spermatids) and somatic cells (Sertoli cells, peritubular myoid cells, Leydig cells, and macrophages), as well as their distinct subsets, annotated on the basis of established biomarkers.

For instance, Sohni and colleagues identified four distinct subsets of human spermatogonia based on transcriptomic profiles: SSC-1, SSC-2, early diff-SPG, and Diff-SPG. MAGEA4 and DDX4 were found to be commonly expressed across all four subsets (Kossack et al., 2013). SSC-1, characterized by UTF1 expression, was identified as the least differentiated subset, representing the SSCs. This subset can be further divided into three groups: SSC-1A, SSC-1B, and SSC-1C. Pseudotime analysis, which traces developmental trajectories based on transcriptomic changes, revealed that SSC-1A, SSC-1B, and SSC-1C are organized in a 'donut-shaped' cluster, with SSC-1B containing the most primitive spermatogonia. SSC-1B can transition to SSC-1A and SSC-1C states before differentiating into Early diff-SPG, suggesting that SSC-1 subsets exhibit high plasticity. Under specific stimuli, these subsets can convert into one another while maintaining a steady-state condition (Sohni et al., 2019) (Fig. 6a).

This plasticity in the most primitive spermatogonia appears to be conserved in non-human primates, as demonstrated by scRNA-seq analysis of *Macaca fascicularis*. Lau and colleagues identified

three subsets of undiff-SPG (Undiff1, Undiff2, and Undiff3) arranged in a 'donut-shaped' configuration, which can transition among each other before differentiation (Lau et al., 2020) (Fig. 6b). The extensive datasets from these studies have also led to the discovery of new germ cell markers, such as NANOS3, which is proposed to be a marker for early differentiating SPG in primates (Lau et al., 2020; Sohni et al., 2019).

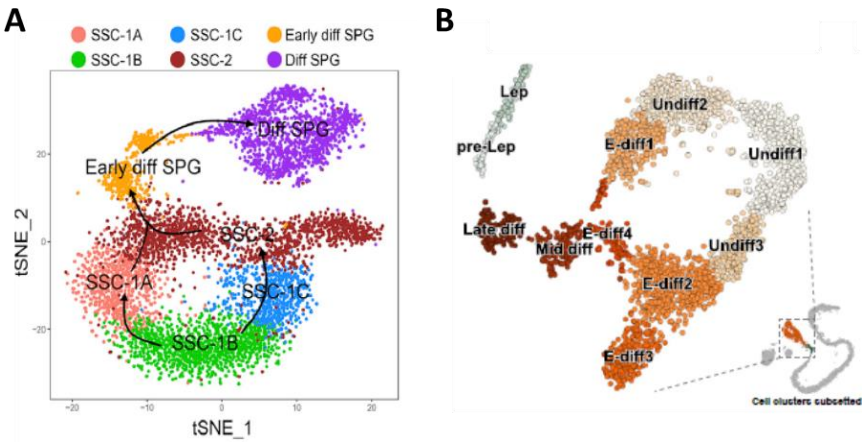

Figure 6: *A) Human spermatogonial subsets identified by scRNA-seq analysis modified (Sohni et al. 2019). B) Monkey spermatogonial subset identified by scRNA-seq analysis (modified from (Lau et al. 2020).*

Recent study noticed that three scRNAseq dataset (Di Persio et al., 2021; Guo et al., 2018; Sohni et al., 2019) reinforced each other by defining analogous undifferentiated cell states, albeit with different nomenclature. Indeed, there were very strong correlations between the expression profiles of each of the three undifferentiated cell clusters, which primarily differed not in the identity of the genes they expressed, but in their relative levels of expression (Bush et al., 2024) (Fig. 7).

Guo 2018	Sohni 2019	Di Persio 2021	Marker genes
State 0	SSC-1B	State 0	C19orf84, EGR4, MAGEA4, PIWIL4, TSPAN33, UTF1
State 0	SSC-1A	State 0A	FGFR3, MAGEA4, UTF1
State 0	SSC-1C	State 0B	MAGEA4, NANOS2, UTF1
State 1	SSC-2	State 1	GFRA1, MAGEA4, NANOS3, UTF1
State 2	Diff SPG	State 2	DMRT1, DNMT1, KIT, MAGEA4, MKI67, SOHLH2
State 3	.	State 2	MAGE4, REC8, STRA8
State 4	.	State 3	.

Figure 7: *A list of common biomarkers expressed in different spermatogonial cell state identified in the aforementioned studies (Bush et al., 2024).*

Moreover, single-cell data provide an unprecedented opportunity to explore communications between the soma and germline in the testis. Germline-soma communication is pivotal in maintaining the testicular environment required for spermatogenesis. In mammals, signaling between germ cells and their somatic counterparts involves the exchange of molecular signals via ligand-receptor interactions. These interactions regulate key processes such as stem cell renewal, differentiation, and maturation. Many somatic cells have the potential (i.e., expression of ligands) to communicate with germ cells, supporting an open niche model for the mammalian testis. Different L-R pairs represented somatic-to-germ cell-interaction, conserved among the species has been discovered, indicating that certain mechanisms of germ cell support are fundamental to mammalian reproduction (Shami et al., 2020) (Fig. 8A-B).

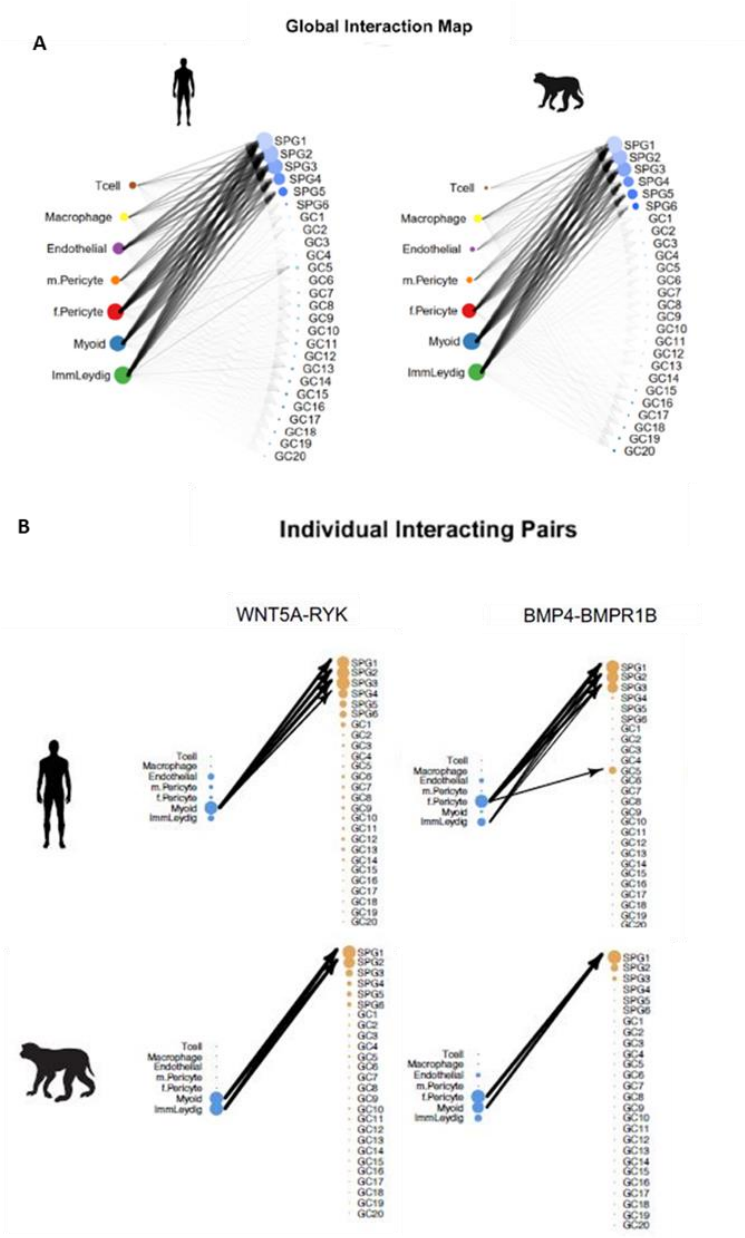

***Figure 8**: A) Summary of the extent of potential interactions between ligands expressed in somatic cells (left) and receptors expressed in germ cells (right),*

Symbol size indicates the number of receptor-ligand interactions contributed by a cell type; and line width shows the number of interactions between the two cell types. B) Pattern of expression for ligand-receptor pairs selected for the present study. Symbol size indicates the level of expression Modified from (Shami et al., 2020).

2.3.3 Localization of spermatogonial stem cell niche

Like other self-renewing adult tissues, the function of the seminiferous epithelium relies on stem cells, specifically SSCs. These SSCs are influenced by various extrinsic signals from the "stem cell niche." The stem cell niche refers to the specialized microenvironment where stem cells reside, playing a crucial role in maintaining tissue homeostasis by balancing the production of stem cells and progenitor cells. This balance is achieved through cell-cell and cell-matrix interactions, as well as signaling molecules that modulate the transcriptional programs within the cells (Voog and Jones, 2010).

The SSC niche is located within the basal lamina of the seminiferous tubules and includes somatic Sertoli cells, which are in close contact with germ cells. Unlike other adult stem cells housed within a "closed" niche, SSCs exist in an "open niche" model. In this model, they are intermingled with progenitor and diff-SPG in the basal compartment of the testis (Yoshida, 2018). Additionally, due to cyclical fluctuations in the expression of paracrine regulators, the nature of the SSC niche changes over the course of the seminiferous epithelial cycle (Mäkelä and Hobbs, 2019). Thus, SSCs are influenced by both their spatial distribution within the seminiferous tubules and the complex interplay of metabolic and molecular signals.

There is limited knowledge about the exact location of SSCs and the spermatogonial stem niche, and whether these aspects are evolutionarily conserved between species. In rodents, it has been

shown that undiff-SPG, identified through histomorphological criteria of the nucleus, are not randomly distributed within the seminiferous tubules. At specific stages of the seminiferous epithelial cycle they are preferentially located in regions of the tubule close to the interstitial areas (Chiarini-Garcia et al., 2001). Subsequently, it was observed that these interstitial areas are characterized by an elevated vascular network, suggesting that the presence of vessels in the interstitium influences the behavior of undiff-SPG (Yoshida et al., 2007). Observational studies using an Id4-eGfp transgenic mouse demonstrated that, unlike progenitors and diff-SPG, the functionally defined ID4-eGFP+ SSC population is typically located in tubule regions that lack contact with the interstitial space (Chan et al., 2014). More recently, oxygen-sensing probes in the same model revealed that the majority of SSCs are found in low-oxygen environments, with EPAS1 (HIF-2α) playing a key role in sustaining their function within these hypoxic conditions (Bernstein et al., 2023). Additionally, an analysis of scRNA-seq datasets from mouse and human testes has shown a conserved upregulation of genes related to mitochondrial function, biogenesis, and oxidative phosphorylation in diff-SPG, while SSCs exhibit a gene expression profile characteristic of glycolytic metabolism (Lord and Nixon, 2020). Taken together, these findings underscore that while hypoxia is crucial for maintaining SSCs, the shift from a stem cell state to progenitor and differentiating cells coincides with relocation to areas of the testes with higher oxygen levels, where hypoxia signaling is diminished.

While the localization of the spermatogonial stem niche and the distribution of the most undiff-SPG in rodents remains a topic of debate, even less is known about primates. The only evidence regarding the distribution of potential SSCs in primates comes from Caldeira and colleagues, who, based on morphological recognition of spermatogonia, proposed that in humans, the most primitive cells, identified as an Adark subpopulation, are preferentially located near blood vessels (Caldeira-Brant et al.,

2020). This finding supports the hypothesis that seminiferous tubule regions in close contact with the interstitium and blood vessels are favorable niches for primitive spermatogonia.

2.3.4 Kinetic of primate spermatogonial compartment

In the non-human primate, the first evidence related to the kinetic of the undifferentiated spermatogonial compartment comes from the studies of Clermont. In 1959, his studies on the undifferentiated spermatogonial compartment of the Macacus Rhesus led him to propose that the Ad spermatogonia are the stem cells while the Ap are the committed progenitors (Clermont et al., 1959). Subsequent observations revealed that in a steady-state condition, Ad SPG did not incorporate H3-thymidine, prompting Clermont to revise his model. He suggested that Ad SPG are "reserve stem cells," remaining mostly quiescent until activated by testicular damage, whereas Ap SPG function as "active stem cells" that self-renew or differentiate into the first generation of diff-SPG (B1 SPG) under normal conditions (Clermont, 1969). Supporting this hypothesis, a study by van Alphen and colleagues in 1988 showed that following germ cell loss induced by testicular irradiation in Rhesus monkeys, the remaining Ad SPG transitioned into Ap SPG, repopulating the testicular tissue (van Alphen et al., 1988). Although this supported the reserve role of Ad SPG, their exact function under steady-state conditions remained unclear. Over the years, several authors identified the Ap division between stage VII and IX (Clermont, 1969; Clermont and Antar, 1973; Fouquet and Dadoune, 1986) although there is disagreement in the literature about whether Ap divide once (Clermont, 1969; Simorangkir et al., 2009) or twice (Clermont and Antar, 1973; Ehmcke et al., 2005) during these stages. Ehmcke et al., in 2005, found two peaks of Ap mitotic activity during the cycle of the seminiferous epithelium and they proposed a new model to explain how the Ap can maintain monkey spermatogenesis while the Ad stay quiescent: the “clone splitting model”. According to this model, clones of eight Ap SPG

produced at stage VII fragment into smaller clones of two or four spermatogonia, which can then divide again at stage IX to form new clones of eight Ap SPG or four to eight B1 SPG (Fig.9) (Ehmcke et al., 2005). The kinetic activity of Ap during the cycle allowed Hermann to propose a parallel between mouse Aal and primate Ad (Hermann et al., 2010). Fouquet & Dadoune showed that in the monkey testis the Ad and the cells with an intermediate phenotype didn't fluctuate during the cycle of the seminiferous epithelium, while the number of Ap had a peak at stage VI-IX (Fouquet and Dadoune, 1986). Therefore, it could be hypothesized that the Ad are similar to As and Apr, the number of which do not change during the cycle, while the Ap resembled Aal, the number of which increase at stage IX-III (Hermann et al., 2010). As for the kinetics of the differentiating spermatogonial compartment in non-human primates, B1 SPG arises from the differentiation of Ap SPG at stage X, followed by a series of stage-specific mitoses at stages XI-II and IV. The last generation of diff-SPG, B4, divides at stage VI to produce preleptotene spermatocytes, which then enter meiosis (Clermont et al., 1959).

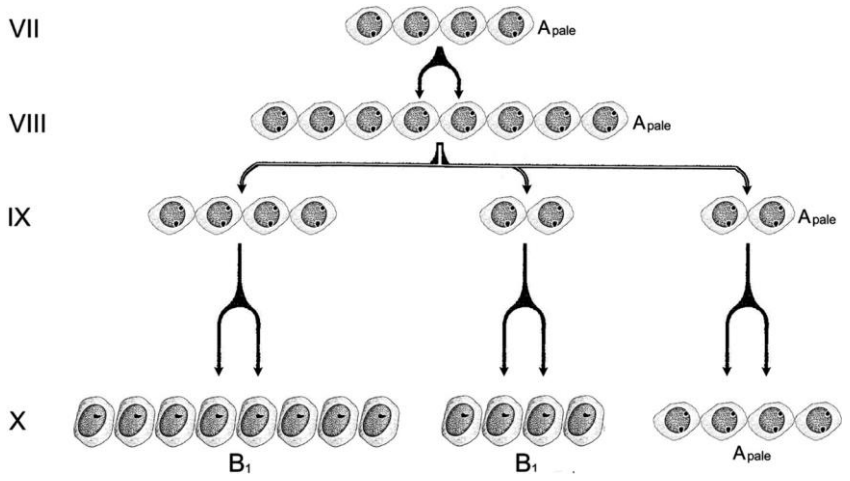

Figure 9**:** *Schematic of the kinetics of proliferation of A-spermatogonia in the rhesus monkey, as proposed by Ehmcke et al. (Ehmcke et al., 2005).*

Recently, the discovery of a novel small SPG population, corresponding to 3% of all MAGEA4+ SPG, led to the proposal of an alternative model for the kinetics of non-human primates spermatogonial compartment, challenging the actual "clone splitting model".
This novel SPG population has particular characteristics: is quiescent but characterized by lower levels of KIT and larger nuclear diameters compared to the stage-specific B spermatogonia, express also low levels of UCHL-1 and medium/high level of MAGEA4 and is localized from stage II to stage VII. It was proposed that these cells represent early differentiating spermatogonia in transition to became B1. During this transition, they re-enter cell cycle, undergo S-phase along with the S-phase of preleptotene spermatocytes (stages VI-VII) and divide at stage VIII to generate B2 (Fig. 10) (Capponi et al., 2023). This model is analogous to the situation in rodents were the first generation of diff-SPG (A1 SPG) are generated by transformation of undiff-SPG (A aligned SPG) without cell division (de Rooij and Russell, 2000; van Pelt and de Rooij, 1991).

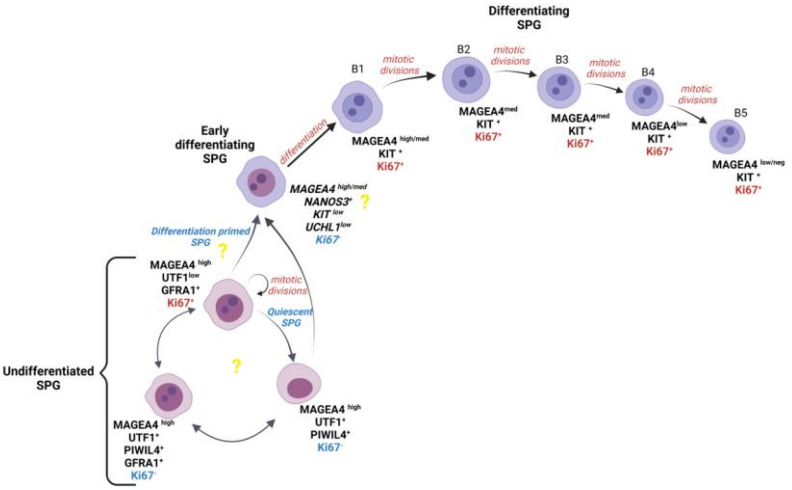

Figure 10**:** *Model for the premeiotic spermatogonial expansion in primates. Modified from (Capponi et al., 2023).*

For humans, Clermont initially proposed a model similar to that of monkeys, suggesting that Ad SPG are stem cells and Ap SPG are committed precursors. He identified two mitotic peaks during the human seminiferous epithelium cycle: at stages V and II. According to his model, at stage V, Ad SPG can either produce two new Ad SPG or two Ap SPG, which at stage V of the next cycle divide to generate B SPG. At stage II, B SPG undergoes a single mitotic division to form preleptotene spermatocytes. Clermont determined the clonal size based on his counts, finding equal numbers of Ap and Ad SPG, and twice as many B SPG per 1,000 Sertoli cells (Clermont, 1966a, b).

Recently, the kinetics of the human spermatogonial compartment was reassessed (Di Persio et al., 2017). It was found that the vast majority (over 95%) of undiff-SPG are quiescent, with mitotic Ap-d SPG being extremely rare, mostly consisting of single cells and occasional pairs, and without chains of mitotic Ap-d SPG. This suggests that in humans, most Ap-d SPG exist as single cells. Although Ap-d SPG proliferate throughout the cycle, their mitotic activity peaks at stage IX. The analysis of mitotic KIT+ B SPG revealed three mitotic peaks at stages IX, II/III, and V/VI, indicating the presence of three generations of B spermatogonia (B1, B2, and B3) rather than just one as previously suggested by Clermont. Additionally, nearly half of the B SPG were not engaged in the cell cycle, contrasting with rodents, where diff-SPG generations are consistently active in the cell cycle. The reasons behind the downregulation of B SPG proliferation in humans are not yet fully understood and warrant further investigation.

3. AIMS

The maintenance of seminiferous epithelium function hinges on the intricate molecular and cellular interactions between SSCs and their cognate niche. To sustain the continuous production of sperm, a delicate balance needs to prevail among the several niche factors that control cell fate decisions of SSCs by promoting self-renewal or spermatogenic commitment of the undiff-SPG. Despite its critical importance, our understanding of SSCs homeostasis remains limited, in particular the spatial distribution of the SSCs within the testicular microenvironment. In rodents it has been shown that undiff-SPG, identified through histomorphological criteria of the nucleus, are not randomly distributed in the seminiferous tubule, but in specific stages of the seminiferous epithelium cycle, they are preferentially located in the areas of the tubule close to the interstitial areas (Chiarini-Garcia et al., 2001). Later it was observed and brought to light how these interstitial areas are characterized by an elevated vascular network, leading to the proposal that the presence of vessels in the interstitium influences the behavior of undiff-SPG (Yoshida et al., 2007). This last aspect has recently been questioned and the new concept of avascular niche would seem to be supported by new evidence obtained through scRNAseq analysis and in vitro SSCs cultures (Bernstein et al., 2023; Lord and Nixon, 2020).

If in rodents the localization of the spermatogonial stem niche and the distribution of the most undiff-SPG is still matter of discussion, even less is it known for primates. The only evidence regarding the distribution of possible SSCs in primates is from Caldeira and colleagues that, based on morphological recognition of spermatogonia, proposed that in humans the most primitive cells, identified as an Adark subpopulation, are located preferentially close to the blood vessels (Caldeira-Brant et al., 2020).

Recently, due to the use of scRNAseq analysis, it has been possible to identify novel spermatogonial markers that are conserved among

primates and are expressed in spermatogonial subsets with stem/progenitor potential (Lau et al., 2020; Sohni et al., 2019).
The goal of the thesis is to better characterize the SSC niche and its regulations in primates.
The specific aims are:
i) The identification of novel putative cell-cell interactions that occur between somatic cells and SSCs that could be crucial for SSC renewal or differentiation in human and non-human primates.
ii) The histological distribution of primate SPG subsets in the seminiferous tubules (i.e. tubule-tubule or tubule-interstitium contact regions) during seminiferous epithelium cycle in primates.

4. RESULTS

4.1 Characterization of putative cell-cell interactions occurring between somatic cells and spermatogonial stem cells

4.1.1 Protein expression of putative Ligand- Rceptor pairs in human and monkey testis sections

To validate the protein expression of ligand-receptor pairs, identified through scRNA-seq analysis (Shami et al., 2020), we decided to perform immunofluorescence analysis for selected L-R pair on testis sections. We selected the ligand-receptor pairs WNT5A-RYK and BMP4-BMPR1B for analysis based on their distinct expression patterns. Specifically, the receptor RYK is expressed exclusively in early spermatogonia (SPG), while its ligand WNT5A is localized to the somatic cells of the testis. Similarly, BMPR1B expression is restricted to early SPG, whereas BMP4 is expressed by somatic cells. These expression patterns were consistently observed across both species, highlighting a potential conserved role for these ligand-receptor interactions in the regulation of early spermatogonia development (Shami et al., 2020). The ligand WNT5A and its receptor RYK were expressed in both species (Fig. 11). RYK immunoreactivity was detected in the cytoplasm of Sertoli cells and Leydig cells in both human (Fig. 11A) and monkey (*Macaca Fascicularis)* (Fig.11B) while WNT5A immunoreactivity was detected in Leydig cells and germ cells in both species (Fig.10A-B). WNT5A immunoreactivity in germ cells showed a restricted distribution in monkey compared to human. WNT5A was detected only in spermatogonia in monkey (Fig. 11B-D) while in human, was detected in all germ cell types (Fig. 11A-C). The distribution of RYK and WNT5A immunoreactivity in the different cell types, are summarized in Fig. 11C (human) and in Fig.11D (monkey).

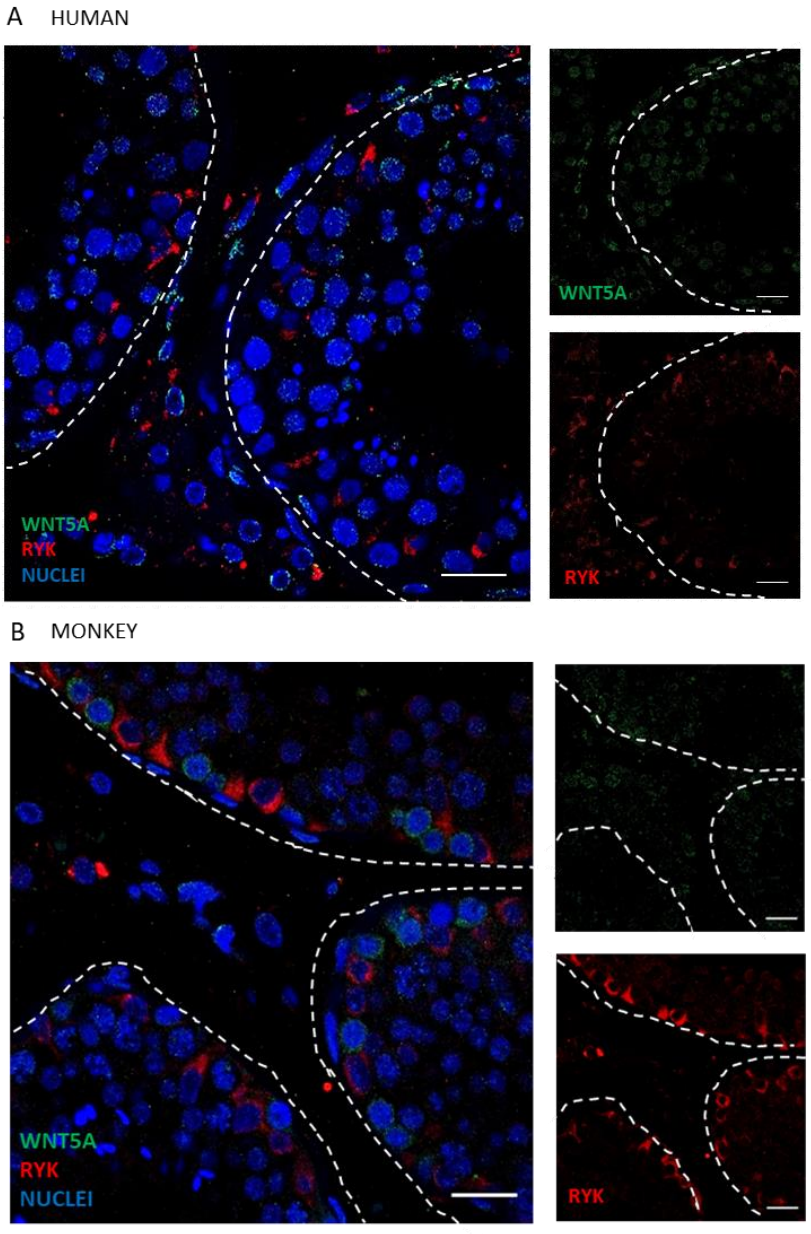
A HUMAN
WNT5A
RYK
NUCLEI
WNT5A
RYK
B MONKEY
WNT5A
RYK
NUCLEI
RYK

C HUMAN

Cell types	WNT5	RYK
Spermatogonia	+++	
spermatocytes	+++	
spermatids	+++	
Sertoli cells		+++
Leydig cells	+++	++

D MONKEY

Cell types	WNT5	RYK
Spermatogonia	+++	
Setoli cells		+++
Leydig cells	++	++

Figure 11: *A) Representative image of WNT5A (green), RYK (red), and nuclei (blue) staining in human testis sections. Scale bars: 20 µm. B) Representative image of WNT5A (green), RYK (red), and nuclei (blue) staining in cynomolgus monkey testis sections. Scale bars: 20 µm. C) Summary table showing the cell types expressing WNT5A and RYK in human testis sections. The number of (+) symbols indicates the relative expression levels. D) Summary table showing the cell types expressing WNT5A and RYK in monkey testis sections. The number of (+) symbols indicates the relative expression levels.*

The ligand BMP4 and its receptor BMPR1B were also detected in both species (Fig. 12). BMP4 immunoreactivity was detected only in the interstitium, specifically by Leydig cells, in both humans and

monkeys. BMPR1B immunoreactivity was detected on cells located at the basal layer of the seminiferous tubule, in both human and monkey. Moreover, in monkey, BMPR1B seems to be expressed very slightly by Leydig cells in the interstitium as well (Fig.12B-D). The different cell types that express BMP4 and BMPR1B are summarized in Fig. 12C (human) and in Fig. 12D (monkey).

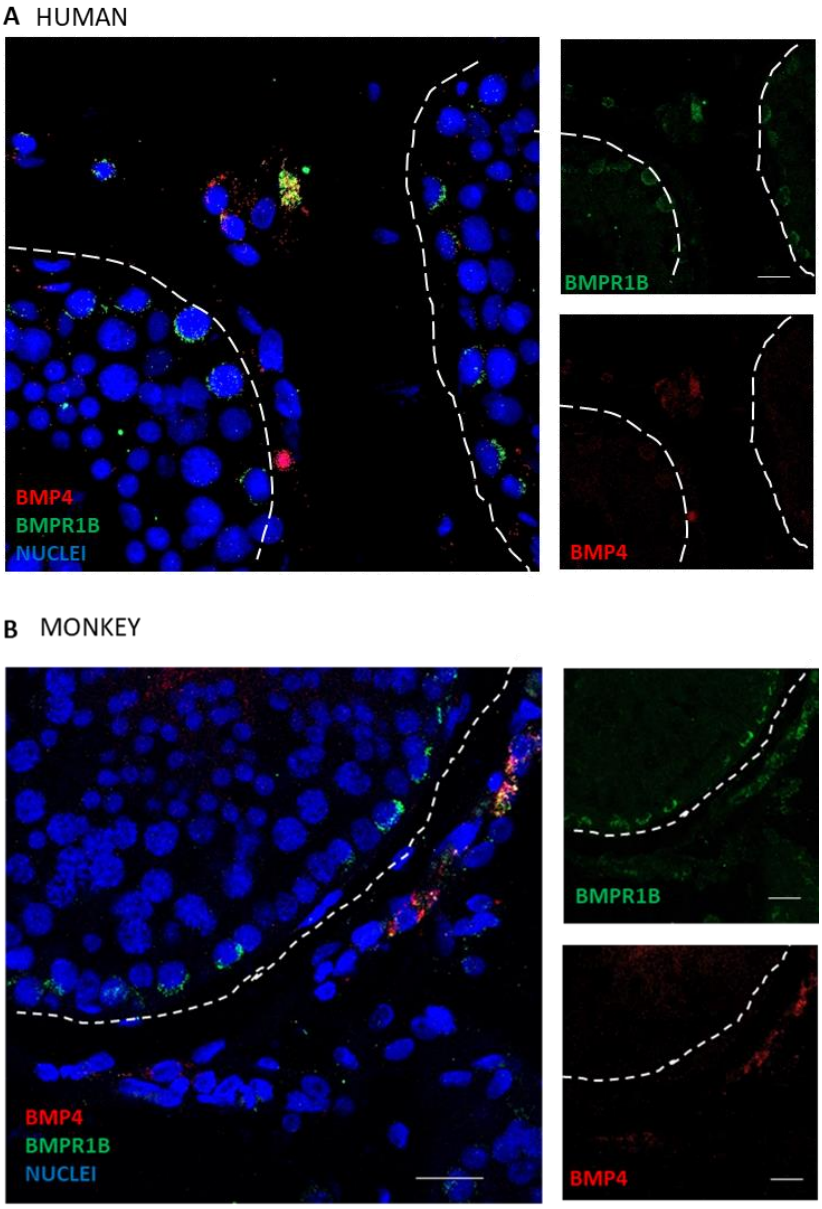
A HUMAN
BMP4
BMPR1B
NUCLEI
BMPR1B
BMP4
B MONKEY
BMP4
BMPR1B
NUCLEI
BMPR1B
BMP4

C HUMAN

Cell types	BMP4	BMPR1B
Spermatogonia		+++
Leydig cells	+++	

D MONKEY

Cell types	BMP4	BMPR1B
Spermatogonia		+++
Leydig cells	+++	+

***Figure 12**: A) Representative image of BMP4 (red), BMPR1B (green), and nuclei (blue) staining in human testis sections. Scale bars: 20 µm. B) Representative image of BMP4 (red), BMPR1B (green), and nuclei (blue) staining in cynomolgus monkey testis sections. Scale bars: 20 µm. C) Summary table showing the cell types expressing BMP4 and BMPR1B in human testis sections. The number of (+) symbols indicates the relative expression levels.D) Summary table showing the cell types expressing BMP4 and BMPR1B in monkey testis sections. The number of (+) symbols indicates the relative expression levels.*

The results showed that for the L-R pair WNT5A-RYK, the RNA and protein expression do not fully correlate. On the contrary, the protein expression profile of the L-R pair BMP4-BMPR1B correlates with scRNA-seq data in both humans and monkeys (Shami et al., 2020).

4.1.2 Histological distribution of the specific cell types expressing BMP4-BMPR1B Ligand-Rceptor pair.

Since the protein expression of the BMP4-BMPR1B pair correlates with scRNA-seq data, we decided to further characterize the cell types expressing BMP4 and BMPR1B, and their histological distribution. We performed immunohistochemistry (IHC) on Bouin-fixed specimens, which better preserve morphology and allow for the recognition of the different cell types present in the seminiferous tubules. IHC confirmed that BMP4 is expressed by Leydig cells in both human (Fig. 13A-B) and monkey (Fig. 13C-D), and that $BMPR1B^{+}$ are the SPG lying on the basal lamina of the seminiferous tubules in both species. Interestingly, only in monkey is BMPR1B also expressed in the interstitium by Leydig cells. The frequency of $BMPR1B^{+}$ SPG was high in both species, with positive cells detected on the basal lamina of the seminiferous tubules in almost every cross-section (Fig. 13B-D).

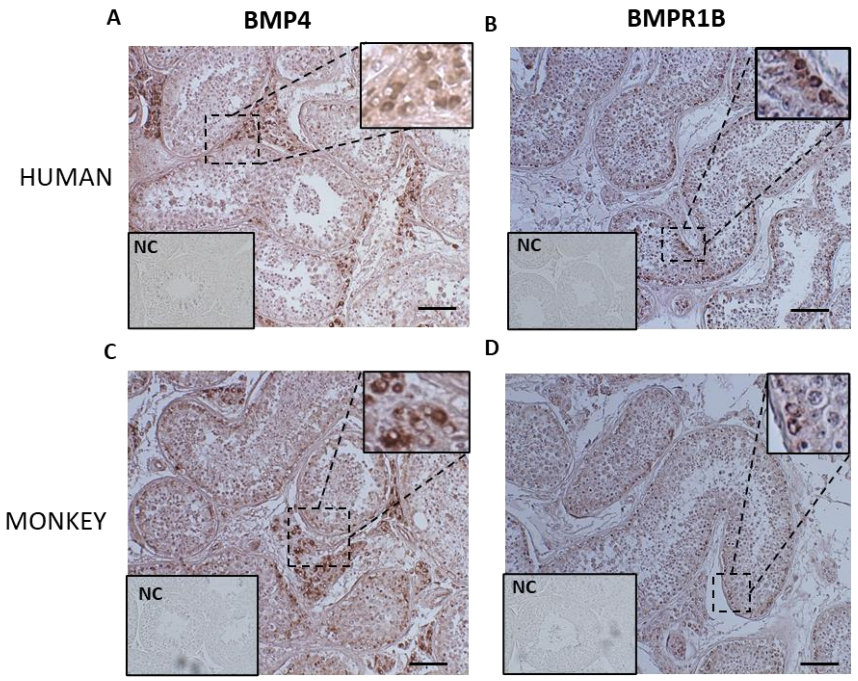

Figure 13: *A-B) Representative images of BMP4 (left) and BMPR1B (right) immunohistochemistry in human testis sections. Insets show examples of positive cells. NC: negative control. Scale bars: 50 µm. C-D) Representative images of BMP4 (left) and BMPR1B (right) immunohistochemistry in monkey testis sections. Insets show examples of positive cells. NC: negative control. Scale bars: 50 µm.*

4.1.3 Characterization of the specific cell types expressing BMPR1B in monkeys whole mounted tubules.

To further pinpoint which spermatogonial type expressed BMPR1B, we co-stained monkey whole-mounted seminiferous tubules with BMPR1B and well-stablished SPG markers. We first analyzed its expression overlap with UCHL-1, a marker for all undiff-SPG cells (Tokunaga et al., 1999) (Fig. 14A). The results show that most UCHL-1$^+$ were also positive for BMPR1B (80%), with a small percentage of BMPR1B-positive cells that were not UCHL-1$^+$ (3%) (Fig. 14B). The observation of BMPR1B$^+$/UCHL$^-$ SPG prompted us to ask if this subset could comprise part of diff-SPG. Therefore, we performed double immunofluorescence using KIT, a marker for diff-SPG, alongside BMPR1B. The results confirmed that, despite almost all the differentiated SPG being negative for BMPR1B (~77%), a small percentage of KIT$^+$ SPG, around 3%, co-expressed BMPR1B (Fig. 14C-D).

In cynomolgus monkeys, as in humans, the undiff-SPG display high phenotypic heterogeneity in terms of protein expression, with several subsets identified (Capponi et al., 2023; Di Persio et al., 2017). To further dissect the heterogeneity of BMPR1B-expressing undiff-SPG, we decided to continue the characterization using other known markers for undiff-SPG, such as GFRA1 and PIWIL4 (Boitani et al., 2016; Di Persio et al., 2021; Sohni et al., 2019). First, we performed double staining with BMPR1B and PIWIL4 on monkey intact tubules to quantify the BMPR1B$^+$/PIWIL4$^+$ SPG (Fig. 14E). The results indicate that most SPG were positive only for BMPR1B (around 70%), while all the PIWIL4$^+$ SPG co-expressed BMPR1B (around 30%) (Fig. 14F). Next, we quantified the number of BMPR1B and GFRA1 co-expressing cells (Fig. 14G). The analysis revealed that only 17% of BMPR1B+ spermatogonia (SPG) also expressed GFRA1, while the remaining 83% were exclusively BMPR1B+. Interestingly, all GFRA1+ SPG

were found to co-express BMPR1B, similar to the pattern observed for PIWIL4+ SPG (Fig. 14H).

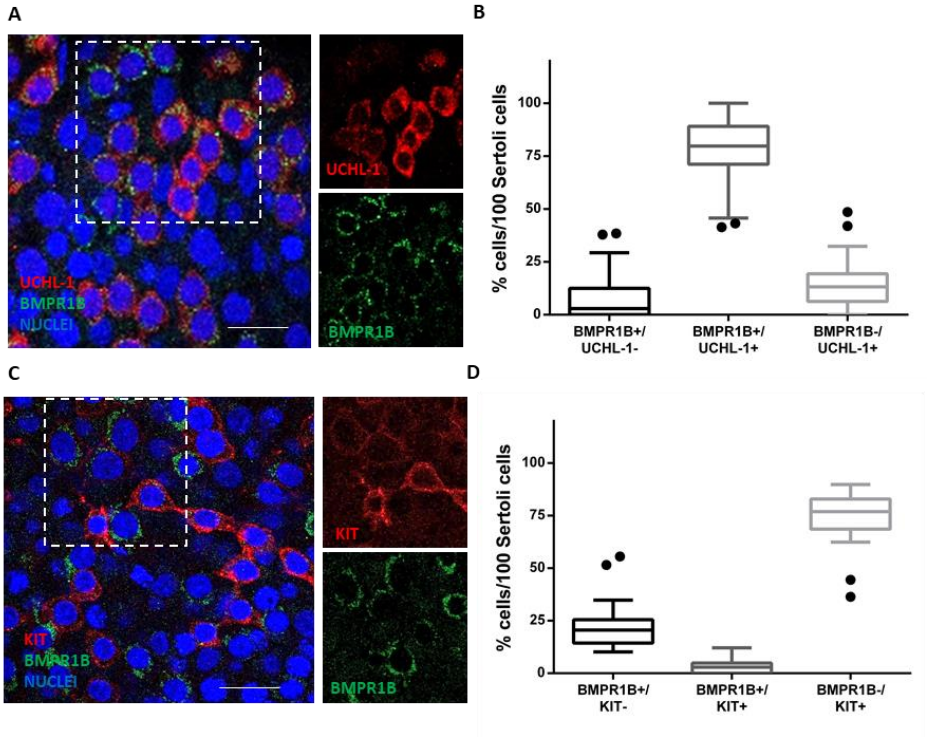

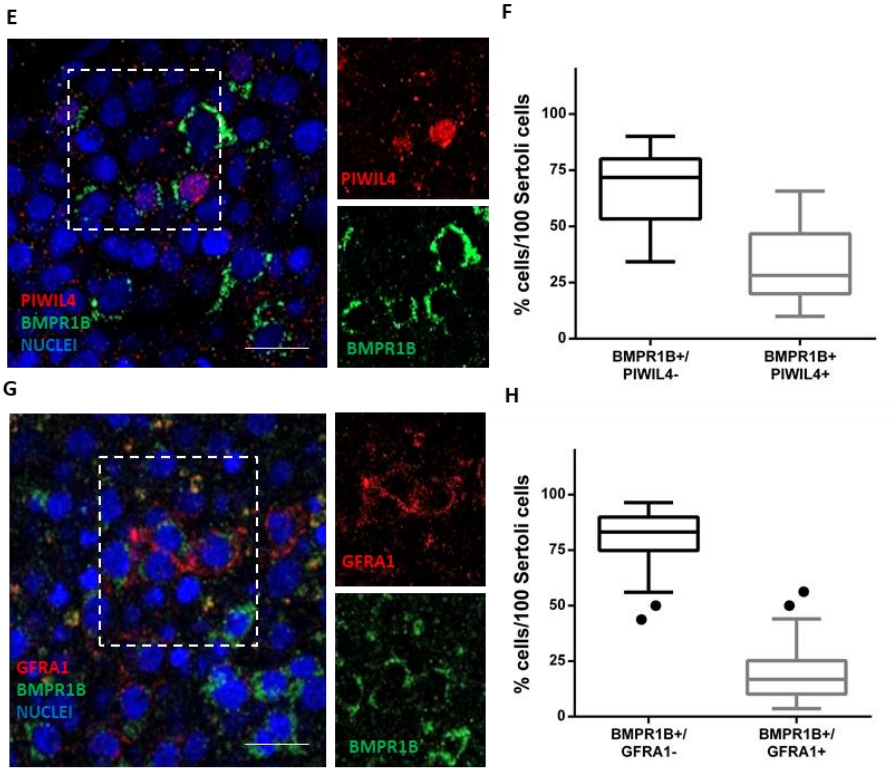

Figure 14: *A) Representative wholemount staining of BMPR1B (green), UCHL-1 (red), and nuclear staining (blue) in monkeys. Scale bars: 20 µm. B) Box plot representing the percentage of BMPR1B^{+}/UCHL-1^{-}, BMPR1B^{+}/UCHL-1^{+}, and BMPR1B^{-}/UCHL-1^{+} SPG in cynomolgus monkey seminiferous tubules. More than 2,400 cells were counted from three samples. C) Representative wholemount staining of BMPR1B (green), KIT (red), and nuclear staining (blue) in monkeys. Scale bars: 20 µm. D) Box plot representing the percentage of BMPR1B^{+}/KIT^{-}, BMPR1B^{+}/KIT^{+}, and BMPR1B^{-}/KIT^{+} SPG in monkey seminiferous tubules. More than 2,000 cells were counted from three samples. E) Representative wholemount staining of BMPR1B (green), PIWIL4 (red), and nuclear staining (blue) in monkeys. Scale bars: 20 µm. F) Box plot representing the percentage of BMPR1B^{+}/PIWIL4^{-} and BMPR1B^{+}/PIWIL4^{+} SPG in monkey seminiferous tubules. More than 1,000 cells were counted from three samples. G) Representative wholemount staining of BMPR1B (green), GFRA1 (red), and nuclear staining (blue) in monkeys. Scale bars: 20 µm. H) Box plot representing the percentage of BMPR1B^{+}/GFRA1^{-} and BMPR1B^{+}/GFRA1^{+} SPG in monkey*

seminiferous tubules. More than 1,500 cells were counted from three samples. Box plot in B,D,F and H are defined as follows: center line: median; box limits: upper and lower quartiles; whiskers: 1.5 x interquartile range; points: outliers.

4.1.4 Characterization of the specific cell types expressing BMPR1B in human whole mounted tubules.

Since we know that SPG progression, based on protein markers, is conserved in human and monkey, we asked whether BMPRB1 expression identifies similar SPG subsets also in human (Capponi et al., 2023) by performing the same co-staining on intact human seminiferous tubules (Fig. 15). The results indicate that the percentage of $BMPR1B^{+}/UCHL\text{-}1^{+}$ SPG is lower in humans compared to monkeys (46,5% vs 80%). Moreover, we also found a subset of $BMPR1B^{+}/ UCHL\text{-}1^{-}$ SPG, suggesting they are not undiff-SPG (Fig. 15A-B). Consistently, the co-staining with BMPR1B and KIT revealed the presence of around 19% of $BMPR1B^{+}/KIT^{+}$, indicating that BMPR1B is expressed also in diff-SPG (Fig. 15C- D).

The co-staining with BMPR1B and PIWIL4 shows that, unlike in monkeys, in human BMPR1B is not expressed by all $PIWIL4^{+}$ SPG. Indeed, about 24% of SPG were $BMPR1B^{-}/PIWIL4^{+}$, around 35% were $BMPR1B^{+}/PIWIL4^{+}$, and 40% were $BMPR1B^{+}/PIWIL4^{-}$ (Fig. 15E-F). The presence of three different subsets of SPG was also observed in co-staining of BMPR1B with GFRA1, where 35% of SPG were $BMPR1B^{-}/GFRA1^{+}$, 14% were $BMPR1B^{+}/GFRA1^{-}$, and 47% co-expressed both BMPR1B and GFRA1 (Fig. 15H). These results are in line with a larger proportion of the undiffì-SPG in humans compared to monkeys (Capponi et al., 2023; Di Persio et al., 2017).

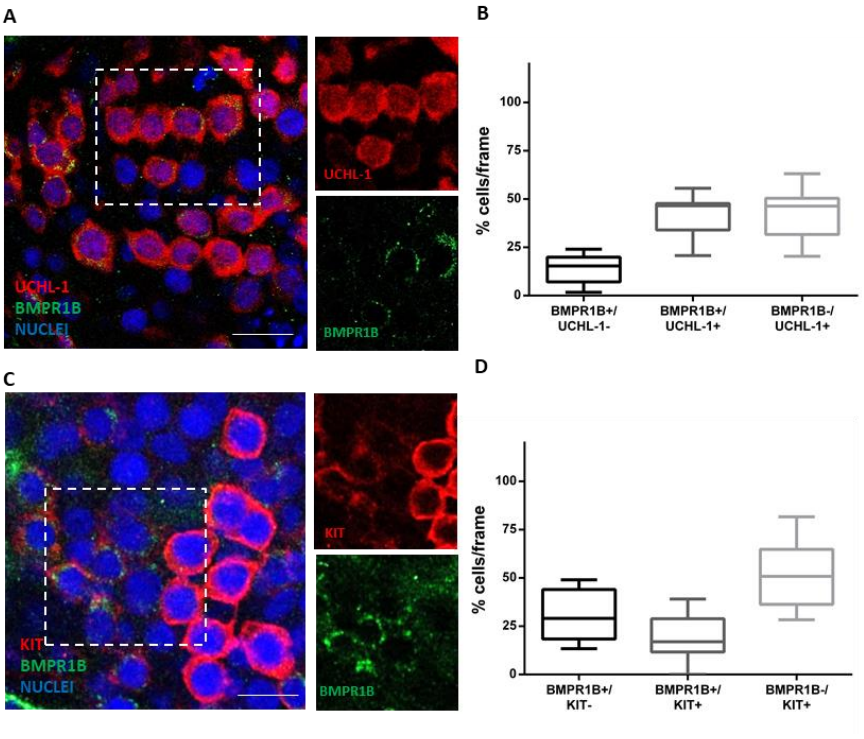
A
UCHL-1
BMPR1B
NUCLEI
UCHL-1
BMPR1B
B
% cells/frame
100
75
50
25
0
BMPR1B+/
UCHL-1-
BMPR1B+/
UCHL-1+
BMPR1B-/
UCHL-1+
C
KIT
BMPR1B
NUCLEI
KIT
BMPR1B
D
% cells/frame
100
75
50
25
0
BMPR1B+/
KIT-
BMPR1B+/
KIT+
BMPR1B-/
KIT+

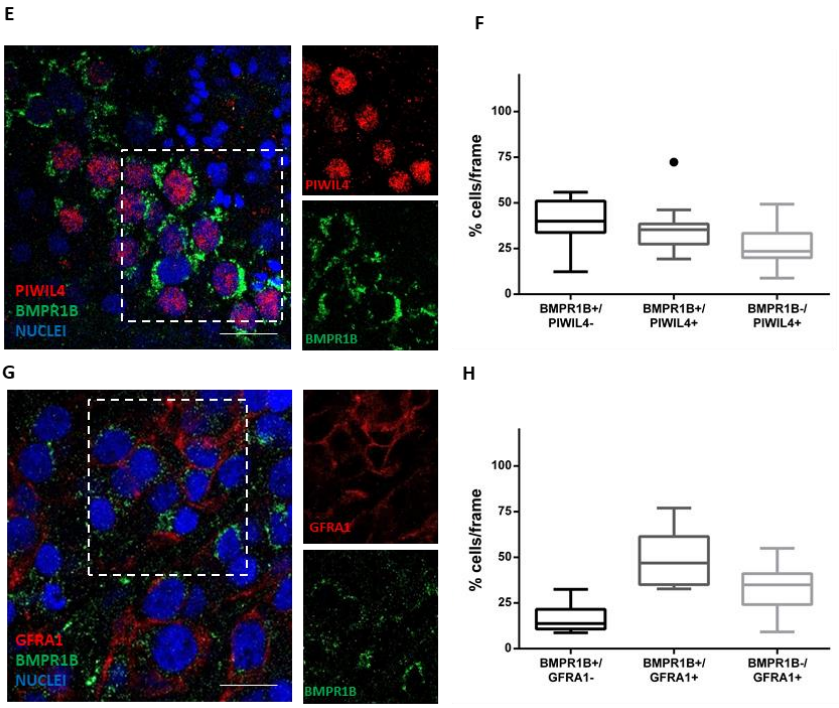

Figure 15: *A) Representative wholemount staining of BMPR1B (green), UCHL-1 (red), and nuclear staining (blue) in human. Scale bars: 20 µm. B) Box plot representing the percentage of BMPR1B^{+}/UCHL-1^{-}, BMPR1B^{+}/UCHL-1^{+}, and BMPR1B^{-}/UCHL-1^{+} SPG in human seminiferous tubules. More than 600 cells were counted from one sample. C) Representative wholemount staining of BMPR1B (green), KIT (red), and nuclear staining (blue) in human. Scale bars: 20 µm. D) Box plot representing the percentage of BMPR1B^{+}/GFRA1^{-}, BMPR1B^{+}/KIT^{+}, and BMPR1B^{-}/KIT^{+} SPG in human seminiferous tubules. More than 700 cells were counted from one sample. E) Representative wholemount staining of BMPR1B (green), PIWIL4 (red), and nuclear staining (blue) in human. Scale bars: 20 µm. F) Box plot representing the percentage of BMPR1B^{+}/PIWIL4^{-} and BMPR1B^{+}/PIWIL4^{+} SPG in human seminiferous tubules. More than 1,100 cells were counted from one sample. G) Representative wholemount staining of BMPR1B (green), GFRA1 (red), and nuclear staining (blue) in human. Scale bars: 20 µm. H) Box plot representing the percentage of BMPR1B^{+}/GFRA1^{-} and BMPR1B^{+}/GFRA1^{+} SPG in human seminiferous tubules. More than 1,700 cells were counted from one sample. Box*

plot in B,D,F and H are defined as follows: center line: median; box limits: upper and lower quartiles; whiskers: 1.5 x interquartile range; points: outliers.

4.1.5 The kinetics of BMPR1B spermatogonia in monkey

To learn more about the proliferative activity of BMPR1B$^+$ SPG, we analyzed MKI67 expression during the cycle of the seminiferous epithelium using monkey seminiferous tubules. MKI67 is marker of cells in all phases of the cell cycle except G0 (Scholzen and Gerdes, 2000).

Initially, we investigated the proliferative activity of BMPR1B$^+$ undiff-SPG. Considering that GFRA1 is the only undiff-SPG marker associated with proliferation in both humans and monkeys (Capponi et al., 2023; Di Persio et al., 2017), we performed a triple immunostaining with BMPR1B, GFRA1, and MKI67, focusing on the spermatogonial subset that co-expresses both BMPR1B and GFRA1 (Fig. 16A). Quantitative analysis showed that, as expected, the majority of BMPR1B$^+$ undiff-SPG were quiescent (Fig. 16B) (Capponi et al., 2023; Di Persio et al., 2017). However, a small number of BMPR1B$^+$/GFRA1$^+$ SPG were engaged in the cell cycle, indicated by MKI67 positivity (Fig. 16B). Subsequently we analyzed the distribution of the identified SPG subsets during the cycle of the seminiferous epithelium. To this end intact tubules were concomitantly stained for SPG markers and for ACR to detect the stages of the seminiferous epithelium (Capponi et al., 2023). BMPR1B$^+$/GFRA1$^+$/MKI67$^+$ SPG were detected in all stages of the seminiferous epithelium cycle with an increase at stage VI-IX (Fig. 16C), in line with a previous study (Capponi et al., 2023).

Next, we analyzed the proliferative index of BMPR1B$^+$ diff-SPG by performing a triple immunostaining with BMPR1B, KIT, and MKI67 (Fig. 16D). Quantitative analysis showed that, as expected, most of the BMPR1B$^+$/KIT$^+$ were in an active cell cycle (Fig.

16E). Interestingly, the BMPR1B^{+}/KIT^{+}/MKI67^{-} SPG subset was localized in the first part of the spermatogenic cycle (Fig. 16F).

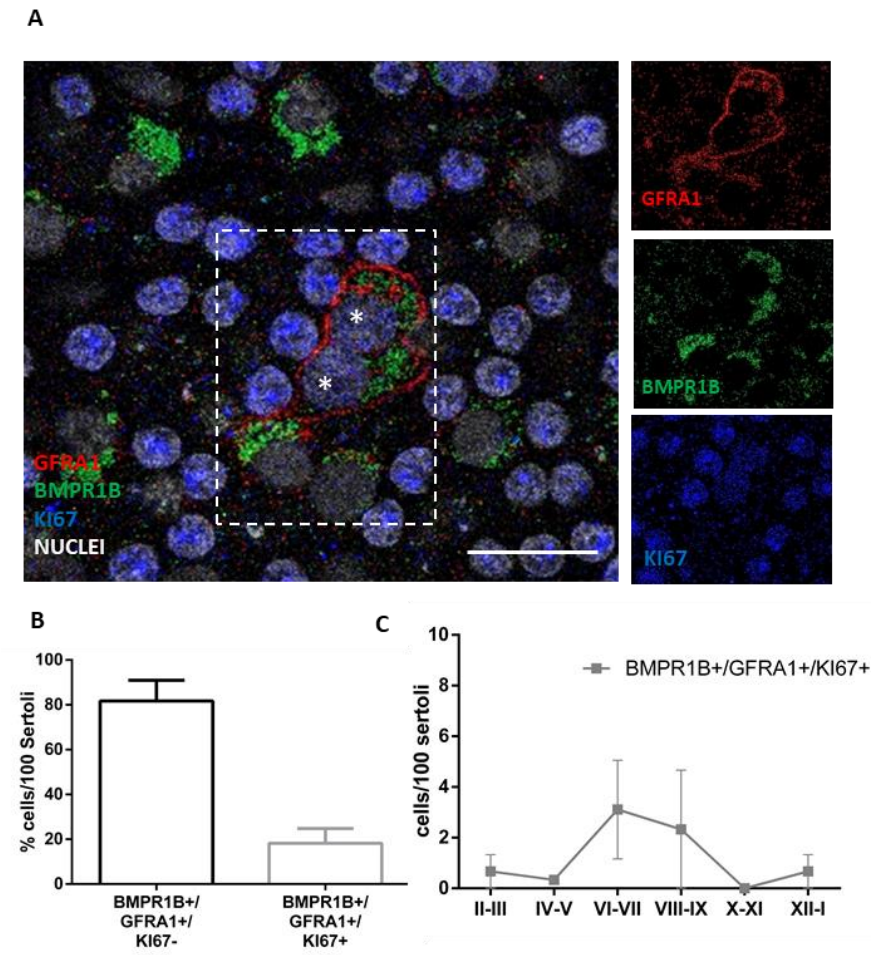

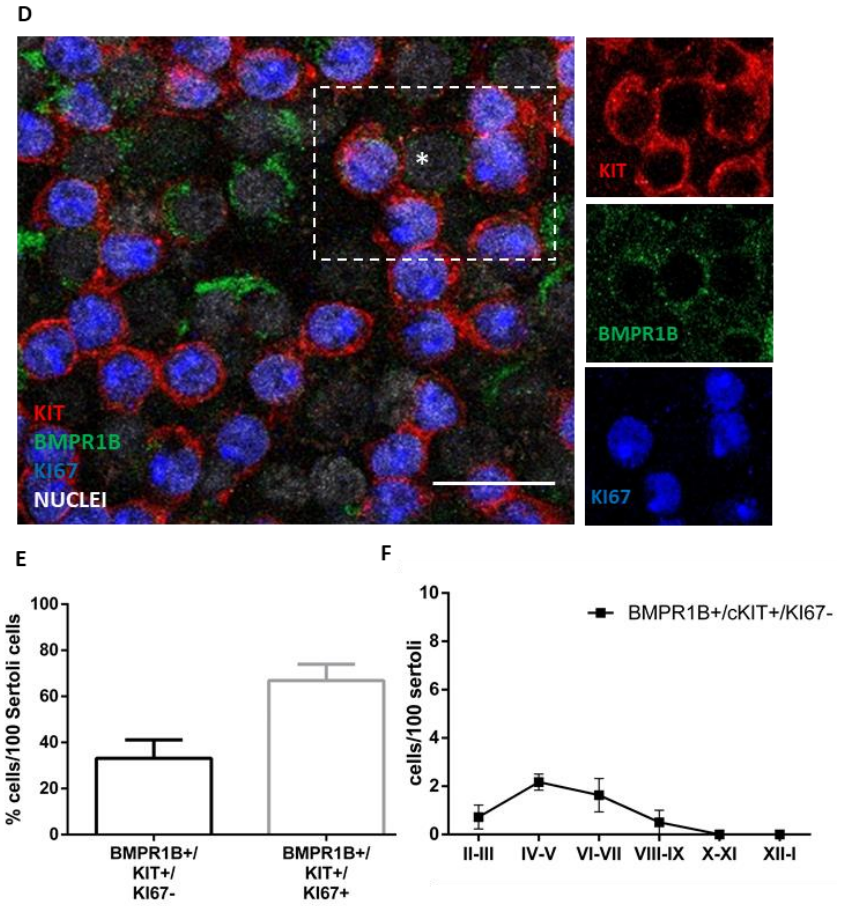

Figure 16: *A) Representative wholemount staining of BMPR1B (green), GFRA1 (red), MKI67 (blue), and nuclear staining (white) in monkeys. Scale bars: 20 µm. B-C) Percentage of BMPR1B^{+}/GFRA1^{+}/MKI67^{-} and BMPR1B^{+}/GFRA1^{+}/MKI67^{+} cells and their distribution across each stage of the seminiferous epithelium cycle. More than 1,000 cells were counted from three samples. D) Representative wholemount staining of BMPR1B (green), KIT (red), MKI67 (blue), and nuclear staining (white) in monkeys. Scale bars: 20 µm. E-F) Percentage of BMPR1B^{+}/KIT^{+}/MKI67^{-} and BMPR1B^{+}/KIT^{+}/MKI67^{+} cells and their distribution across each stage of the seminiferous epithelium cycle. More than 1,500 cells were counted from three samples. In B,C, E and F data are presented as mean ± s.e.m.".*

4.2 Evaluation of the histological distribution of different spermatogonia subpopulation during the seminiferous epithelium cycle.

4.2.1 The topographical localization of undifferentiated spermatogonial subpopulations within the testis parenchyma

We have recently demonstrated that the number of the undiff-SPG expressing PIWIL4 and/or GFRA1 doesn't fluctuate significantly between the stages of the epithelial cycle (Capponi et al., 2023). However, it could be possible that the topographical localization of the different subsets along the basal membrane may differ in relation to the interstitial tissue or to the surrounding seminiferous tubules. We therefore asked whether these subpopulations are randomly located along the basal membrane or, on the contrary, if they tend to occupy specific areas, such as the basal membrane facing the interstitial space, or the tubule-tubule contact area. To this end, we performed IHC staining of selected SPG marker followed by immunofluorescence staining for the acrosin for the detection of the stage of the seminiferous epithelium, on monkey testis sections. First, we analyzed the distribution of $PIWIL4^+$ undiff-SPG (Fig. 17A). In *Macaca fascicularis*, the PIWIL4 immunoreactivity was detected in the nucleus of isolated SPG and, on average, 1.5 $PIWIL4^+$ SPG per round tubule cross-section were detected (Fig. 17B). We next evaluated the percentage of $PIWIL4^+$ SPG localized at tubule-tubule contact points or facing the interstitium for each stage of the seminiferous epithelium cycle (Fig. 17C). The results were analyzed for statistical significance using the Li index (Chiarini-Garcia et al., 2001; Chiarini-Garcia and Meistrich, 2008) (Strauss, 1979). A positive Li value (with a maximum of 1) corresponds to positive selection (preference), a negative Li value (with a minimum of -1) corresponds to negative selection (avoidance), while a Li value around 0 corresponds to a random position. The results show that $PIWIL4^+$ SPG are

randomly distributed over the basal membrane for most of the seminiferous epithelium cycle, without showing any preference for a given region (Fig. 17D).

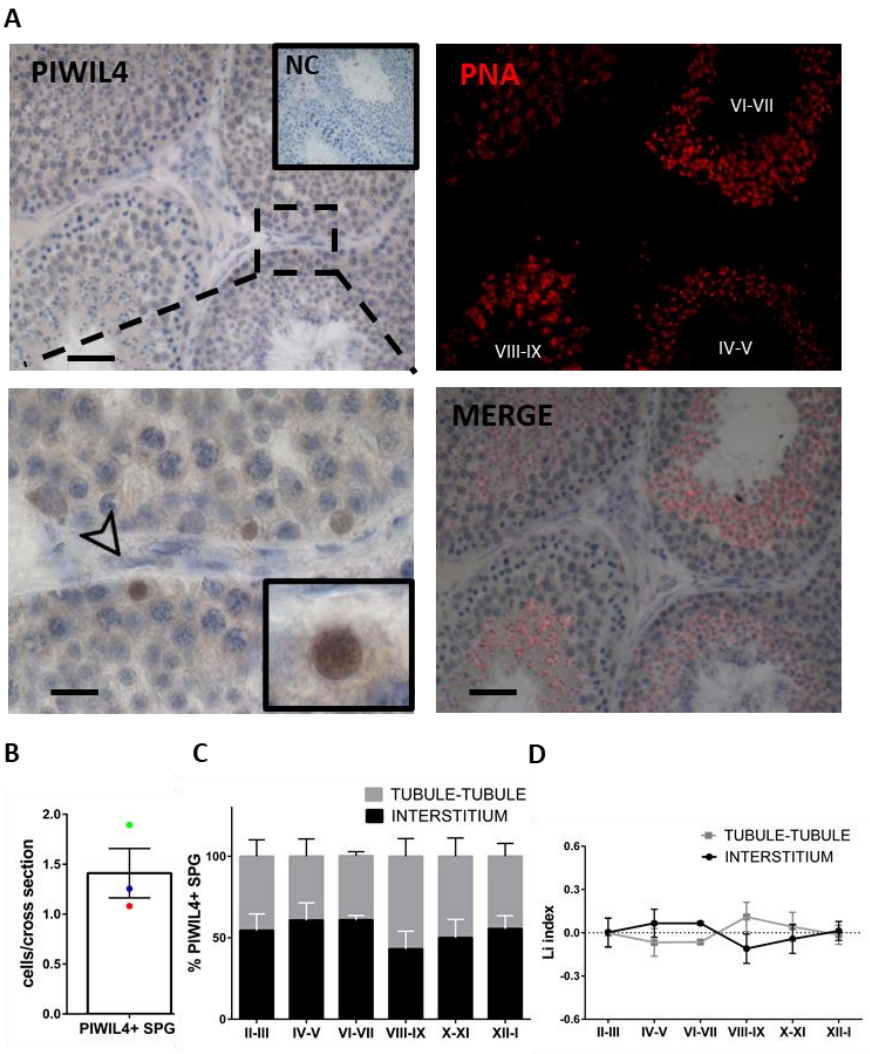

Figure 17: *A) Representative images of IHC staining for PIWIL4 (upper left) and IF staining with PNA (red, upper right) to identify the stage. Negative*

control (NC).The arrow indicates PIWIL4$^+$ undiff- SPG (lower left). The image on the lower right shows a digital merge. Scale bars: 100 µm (upper row). B) Quantification of PIWIL4$^+$ undiff-SPG per round tubule cross-section. A total of 600 cells were scored from n=3 animals. C) Percentage of PIWIL4$^+$ undiff-SPG opposing the interstitial region or the tubule-tubule region along the seminiferous epithelium cycle. D) Li graph showing the distribution of PIWIL4$^+$ undiff-SPG during the seminiferous epithelium cycle. At least 25 round tubule cross-sections were analyzed for each of the 3 animals (total cells counted 192).

We next analyzed the topographical localization of GFRA1$^+$ SPG (Fig. 18). The results indicate that, on average, GFRA1$^+$ SPG were fewer than PIWIL4$^+$ SPG, about 1 for round tubule/tubular cross-section (Fig. 18B). However, the analysis of the histological distribution of GFRA1$^+$ SPG revealed an interesting result. As previously shown, GFRA1$^+$ SPG are present in all stages of the seminiferous epithelium cycle. However, in contrast to PIWIL4$^+$ SPG subset, GFRA1$^+$ SPG subset showed a stage-specific distribution (Fig. 18C). The Li index analysis confirmed that in the first part of the cycle (stage II to VI), GFRA1$^+$ SPG prefer the areas of the tubule facing the interstitial tissue, while in the second half (stages VII to I), they preferentially occupy the basal lamina in tubule-tubule contact areas (Fig. 18D).

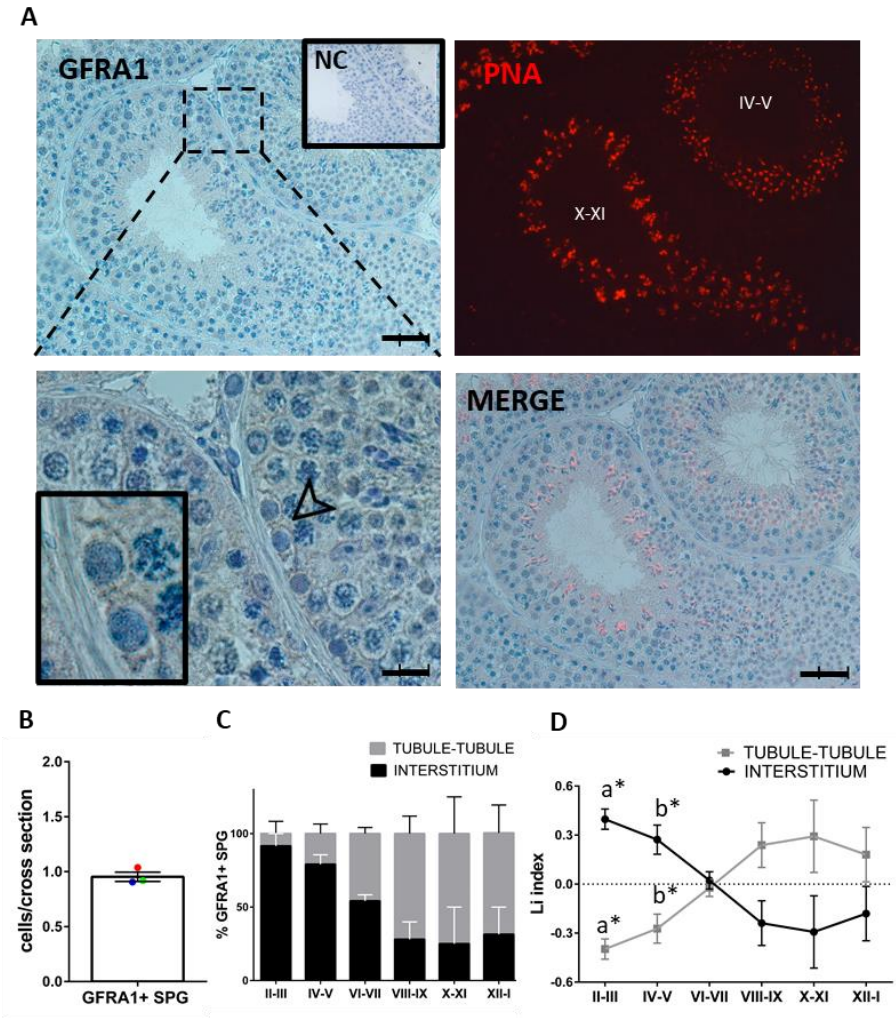

Figure 18: *A) Representative images of IHC staining for GFRA1 (upper left) and IF staining with PNA (red, upper right) to identify the stage. Negative control (NC). The arrow indicates GFRA1⁺ undiff- SPG (lower left). The image on the lower right shows a digital merge. Scale bars: 100 µm (upper row). B) Quantification of GFRA1⁺ undiff-SPG per round tubule cross-section. A total of 350 cells were scored from n=3 animals. C) Percentage of GFRA1⁺ undiff-SPG opposing the interstitial region or the tubule-tubule region along the seminiferous epithelium cycle. D) Li graph showing the distribution of GFRA1⁺*

*undiff-SPG during the seminiferous epithelium cycle. At least 20 round tubule cross-sections were analyzed for each of the 3 animals. (Total cells counted 110). *a= p<0.05 (i.e., p= 0.013 II-III vs. VIII-IX, p= 0.022 II-III vs X-XI, and p= 0.031 II-III vs XII-I); *b=p<0.05 (i.e., p= 0.032 IV-V vs. VIII-IX and p= 0.050 IV vs X-XI).*

4.2.2. The topographical localization of differentiating spermatogonial subpopulations within the testis parenchyma

Among the undiff-SPG, the only fraction of SPG engaged in the cell cycle is the GFRA1$^+$ SPG subset, suggesting that in adult primates, GFRA1 is required to trigger spermatogonial proliferation and to give rise to SPG committed to differentiation (Capponi et al., 2023; Di Persio et al., 2017). Recently, the transcriptome of *Macaca fascicularis* germ cells has been characterized by single-cell RNA sequencing, revealing novel spermatogonial markers, and among these, NANOS3 has been proposed to characterize early stages of spermatogonial differentiation (Lau et al., 2020). To study the histological distribution of SPG committed to differentiation we performed immunohistochemical staining for NANOS3, followed by immunofluorescence for PNA to detect the stage, on monkey testis sections. In positive cells, NANOS3 immunoreactivity showed both a cytoplasmatic and nuclear distribution (Fig. 19A), and cell quantification showed on average 1.3 NANOS3$^+$ SPG per round tubule cross-section (Fig. 19B).

Next, we evaluated the topographical distribution of NANOS3$^+$ SPG with respect to basal membrane facing the interstitial or the tubule-tubule contact area. Like GFRA1$^+$ SPG, the distribution of NANOS3$^+$ SPG on the basal lamina at different stages of the cycle is not random (Fig. 19C). At stages VI-VII, NANOS3$^+$ SPG are preferentially localized in regions of the basal membrane facing the interstitial tissue, while at stages XII-I, they preferentially localize to tubule-tubule contact regions (Fig. 19D).

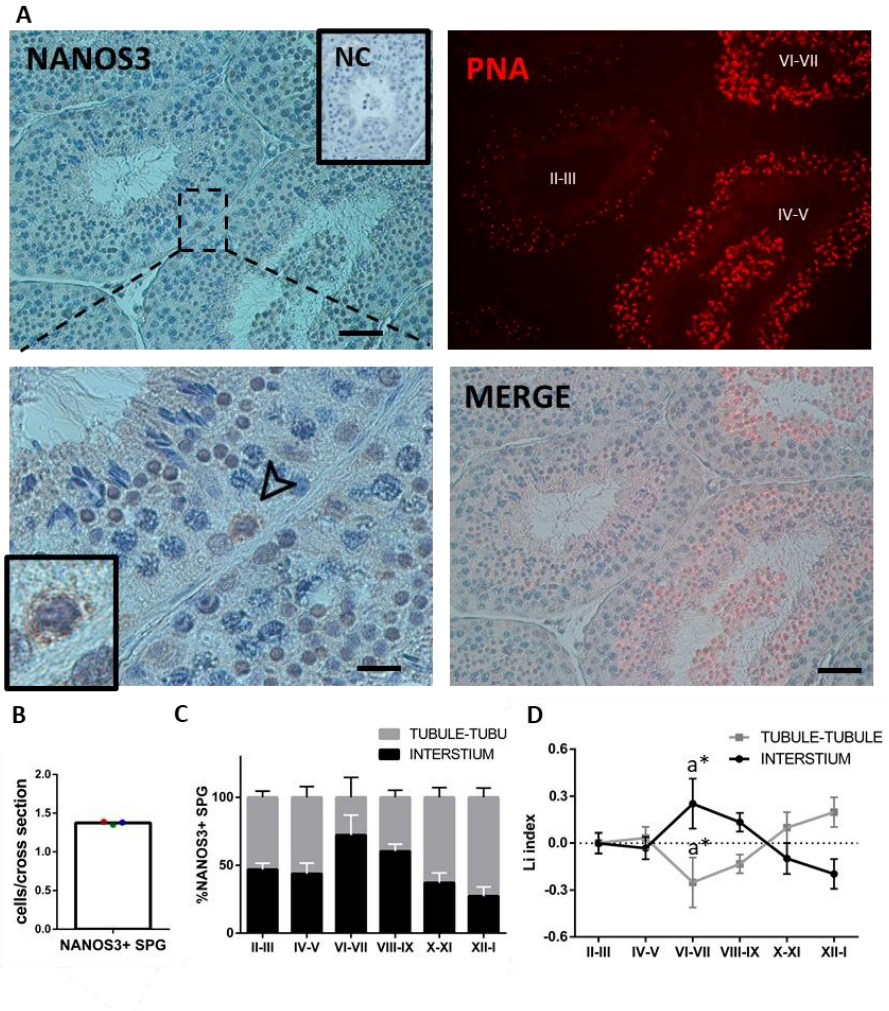

Figure 19: *A) Representative images of IHC staining for NANOS3 (upper left) and IF staining with PNA (red, upper right) to identify the stage. Negative control (NC). The arrow indicates NANOS3⁺ early differentiated SPG (lower left). The image on the lower right shows a digital merge. Scale bars: 100 µm (upper row). B) Quantification of NANOS3⁺ early differentiated SPG per round tubule cross-section. A total of 390 cells were scored from n=3 animals. C) Percentage of NANOS3⁺ early differentiated SPG opposing the interstitial region or the tubule-tubule region along the seminiferous epithelium cycle. D) Li graph showing the distribution of NANOS3⁺ early differentiated SPG during*

*the seminiferous epithelium cycle. At least 30 round tubule cross-sections were analysed for each of the 3 animals (Total cells counted 231). *a= p<0.05 (i.e., P= 0.022 VI-VII vs. XII-I).*

Early diff-SPG are the progenitor cells that give rise to the first generations of Diff-SPG (Sohni et al., 2019). To understand their spatial distribution, we analysed the topographical localization of KIT^+ SPG from stage VI onward, when type B1 SPG first appear, followed by B2 and B3 (Capponi et al., 2023) (Fig. 20A). Histological analysis revealed that, similar to rodents, the first generation of diff-SPG preferentially localize in the interstitial regions during stages VI-VII (Chiarini-Garcia et al., 2001). In contrast, the B2 and B3 generations are randomly distributed, with no specific preference for either tubule-tubule contact zones or interstitium-facing areas (Fig. 20B-C).

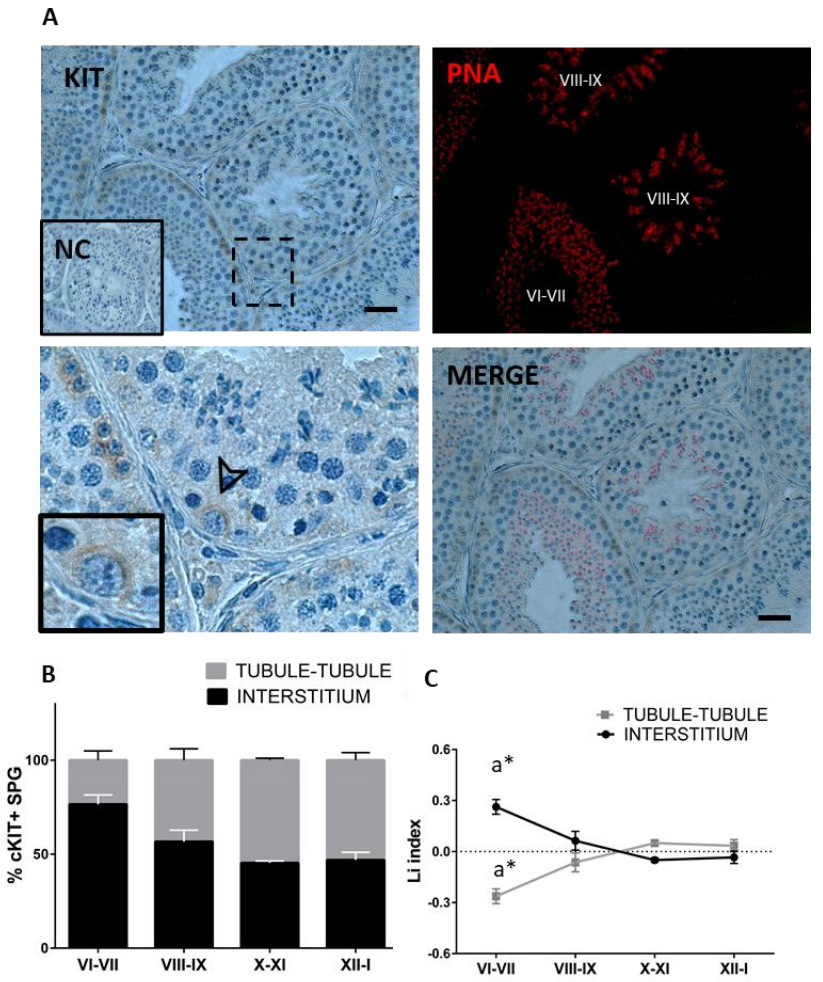

Figure 20 : *A) Representative images of IHC staining for KIT (upper left) and IF staining with PNA (red, upper right) for the identification of the stage. Negative control (NC). The Arrow indicates KIT⁺ diff-SPG (lower left). The image on the lower right shows a digital merge. Scalebars: 100*um *(upper row). B) Percentage of KIT⁺ diff-SPG opposing the interstitial region or the tubule-tubule region along the cycle of the seminiferous epithelium. C) The Li graph for the distribution of KIT⁺ diff-SPG during the cycle of the seminiferous epithelium. At least 20 round tubule- cross sections were analyzed for each of the 3 animals (Total cells counted 289). a*= p<0.05 (i.e., p= 0.006 VI-VII vs VIII-IX, p= 0.05 VI-VII vs X-XI and p= 0.003 VI-VII vs XII-I*

5. DISCUSSION

In many tissue, homeostasis is maintained by physical contact between the stem cell and an anatomically defined niche, however, the identification of SSC niche in mammals has been elusive because the cells are motile and dispersed among their progenies (Morrison and Spradling, 2008; Stine and Matunis, 2013; Yoshida, 2020). In this study, we aimed to gain initial insight into different aspects of the SSC niche in primates, by validating possible niche-derived signaling molecules and by analyzing the topological distribution of different spermatogonial subpopulations along the basal membrane of the seminiferous tubules.

To uncover novel crucial factors involved in the maintenance or differentiation of the early SPG in primate, we took advantage of a ligand-receptor (L-R) bioinformatic analysis, a computational and data-driven examination of interactions between ligands and their corresponding receptors (Shami et al., 2020). However, since mRNA levels do not always correlate with protein abundance, to confirm the relevance of computational predictions, we validated at protein level the expression of ligands and receptors on the predicted cell types.

For the WNT5A-RYK pair, scRNAseq analysis indicated RYK expression in germ cells and WNT5A in the somatic cells of the testis, in both human and monkey. However, RYK was found to be expressed in Sertoli cells and Leydig cells, and not in germ cells as predicted by computational analysis (Shami et al., 2020). These results underscore the importance of protein validations to confirm the biological relevance of the computational predictions.

As for the BMP4-BMPR1B pair, evidence suggests that these proteins play important roles in regulating spermatogenesis in rodents. BMP4, a member of the TGF-β superfamily, signals through type 1 and type 2 BMP receptors, affecting downstream SMAD transducers (Schmierer and Hill, 2007). Studies indicate that BMPs are crucial in male reproduction (Pellegrini et al., 2003; Puglisi et al., 2004; Zhao et al., 1996), with BMP4 specifically

shown to be essential for fertility. In rodents, heterozygous mutations of BMP4 lead to reduced fertility or infertility (Hu et al., 2004). BMP4 facilitates the transition of undiff-SPG to diff-SPG by inducing c-kit expression (Carlomagno et al., 2010; Pellegrini et al., 2003). Additionally, BMP4 is expressed in Leydig cells and negatively regulates their development and regeneration (Li et al., 2022). In contrast, data on BMPR1B is limited, but recent findings suggest it regulates testosterone production and steroidogenesis, influencing Leydig cell function and enzyme expression in a developmentally controlled manner (Ciller et al., 2023).

In the present study, the ligand BMP4 was found to be expressed by Leydig cells in the interstitial tissue, while the receptor BMPR1B was found to be expressed by spermatogonia as predicted by the L-R bioinformatic analysis (Shami et al., 2020). Interestingly, in the monkey, BMPR1B is expressed in almost all the undiff-SPG, while in human BMPR1B does not capture all undiff-SPG, as indicated by detection of $GFRA1^{+}/BMPR1B^{-}$ and $PIWIL4^{+}/BMPR1B^{-}$ SPG. These data align with previous observations showing a differing proportion of the $GFRA1^{+}$ SPG subset within the undiff-SPG compartment in humans and monkeys, which may be attributed to transcriptional profile differences or varying rates of mRNA/protein stability between the two species (Capponi et al., 2023; Di Persio et al., 2017). Furthermore, in analogy to UCHL1, another marker for undiff-SPG, BMPR1B was also co-expressed with KIT in a small percentage of SPG, in both species (Capponi et al., 2023; Di Persio et al., 2017).

The analysis of the proliferative index of $BMPR1B^{+}$ SPG during the seminiferous epithelial cycle indicated that most of $BMPR1B^{+}/GFRA1^{+}$ SPG are quiescent ($MKI67^{-}$) and that along the cycle the $BMPR1B^{+}/GFRA1^{+}/MKI67^{+}$ SPG increase at stages IV-IX, as already shown (Capponi et al., 2023; Di Persio et al., 2017). In this analysis, we also found that the $BMPR1B^{+}/KIT^{+}/MKI67^{-}$ are present in the first half of the cycle. This data suggests that BMPR1B is expressed by the early diff-

SPG, that were recently identified in primates (Capponi et al., 2023).

Taken together, our data show for the first time that in primates, BMPR1B is a marker for almost all the undiff-SPG and also for early diff-SPG.

Among the L-R pairs selected in the presented study (BMP4-BMPR1B and WNT5A-RYK), a positive mRNA-protein correlation was found only for the BMP4-BMPR1B pair, both in human and monkey. While BMP4 and its receptor BMPR1B have been implicated in key processes of spermatogenesis in rodent models, there is no data on how these mechanisms could be translated to primates. The functional validation of the BMP4-BMPR1B interaction *in vivo* and its role in regulating spermatogenesis in primates remains an area requiring further research.

In the mammalian testis, SSCs, progenitor spermatogonia, and diff-SPG are located along the basement membrane of the seminiferous tubules. In rodents, it is well established that the localization of spermatogonia along the basal membrane is non-random and varies with the stage of the cycle and the presence of interstitial tissue (Chiarini-Garcia et al., 2001; Yoshida et al., 2007). In the present study, for the first time, we provide histological evidence of a non-random distribution of spermatogonial subsets during the stages of the seminiferous epithelium cycle in primates. By following the topographical distribution of undiff-SPG along the basement membrane, we found that PIWIL4$^+$ SPG are randomly distributed in all stages of the cycle, i.e. they do not show a preference for regions of the tubule facing other tubules or the interstitial tissue. On the contrary, in the first half of the cycle, GFRA1$^+$ SPG are preferentially located in area of the tubules facing the interstitial tissues while in the second half of the cycle, they preferentially occupy the basal lamina in tubule-tubule contact. Considering that we have previously shown that among all undiff-SPG, only those expressing GFRA1 proliferate (Capponi et al., 2023; Di Persio et

al., 2017), we speculate that their relative position along the basal lamina may regulate their proliferation index.

It is noteworthy that GFRA1^{+} SPG predominantly face the interstitial area during stages II-V, when they exhibit a lower proliferative rate, while their proliferative index increases from stages VI to I, as they are located at tubule-tubule interfaces (Capponi et al., 2023). This suggests that signals from the interstitial area may keep the GFRA1-expressing SPG adjacent to it in a quiescent state, while those further away are able to proliferate, expanding the pool of SSCs and the spermatogonia primed for differentiation.

Nanos3 is an RNA-binding protein that play essential roles during male germ cell development (Inoue et al., 2022; Suzuki et al., 2009). Recently, NANOS3 was identified as a marker for early diff-SPG by scRNAseq both in human (Sohni et al., 2019) and monkey (Lau et al., 2020). Monocle pseudotime trajectory analysis, which aligns individual cells along a developmental trajectory, showed that early diff-SPG give rise to diff-SPG (Sohni et al., 2019). In the present study, we analyzed the topographical arrangement of both NANOS3^{+} SPG and the first generation of diff-SPG, i.e B1 SPG at stage VI-VII (Capponi et al., 2023). By IHC analysis we found that NANOS3^{+} SPG are present in all the stages of the seminiferous epithelium cycle. Interestingly, while NANOS3^{+} SPG are uniformly distributed in most of the stages, at stage VI-VII most of them were found close to regions facing the interstitial tissue, as the B1 SPG, the first generation of diff-SPG. These data suggest that the transition between early diff-SPG and diff-SPG occurs in cells facing the interstitial tissue at stage VI-VII. Moreover, in line with data in mice, we found that while the first generation of diff-SPG preferentially reside in regions adjacent to interstitial tissue, B2 and B3 SPG are randomly distributed along the basement lamina (Chiarini-Garcia et al., 2001).

Analysis of scRNA-seq data from mouse and human showed that diff-SPG upregulate genes associated with mitochondrial function

and oxidative phosphorylation, whereas SSCs show a gene expression profile indicative of glycolytic metabolism (Lord and Nixon, 2020). This suggests that oxygen levels influence spermatogonial cell fate, associating SSCs with hypoxia and differentiating cells with normoxia. Additionally, spermatogonial cell fate may also be influenced by their proximity to growth factors or cytokines produced in the interstitial space (DeFalco et al., 2015; Kitadate et al., 2019).

Our data supports the idea that in non-human primates, progenitor and early diff-SPG are more likely to reside in areas of the basement membrane adjacent to the interstitial space containing the testicular vasculature, although further studies are necessary to characterize the factors and signals involved.

In conclusion, building on these findings regarding the histological localization of undiff-SPG, early diff-SPG and diff-SPG (Fig. 21A), we propose a tentative model for position-dependent spermatogonial progression in adult primates taking into consideration the relationship among spermatogonial subsets during steady-state spermatogenesis and the complex transition highlighted in scRNA-seq studies (Fig. 21B) (Capponi et al., 2023; Di Persio et al., 2021; Lau et al., 2020; Sohni et al., 2019). We propose that, within the pool of quiescent $GFRA1^{+}$ spermatogonia located near the interstitial tissue during the first half of the cycle, some are committed to differentiation and eventually become $NANOS3^{+}$ spermatogonia by stage VI (Fig. 21A-B). At stages VI-VII, these early diff-SPG adjacent to the interstitium begin to lose NANOS3 expression and acquire KIT expression, leading to the formation of the first generation of diff-SPG, at stage VII (Fig. 21A-B).

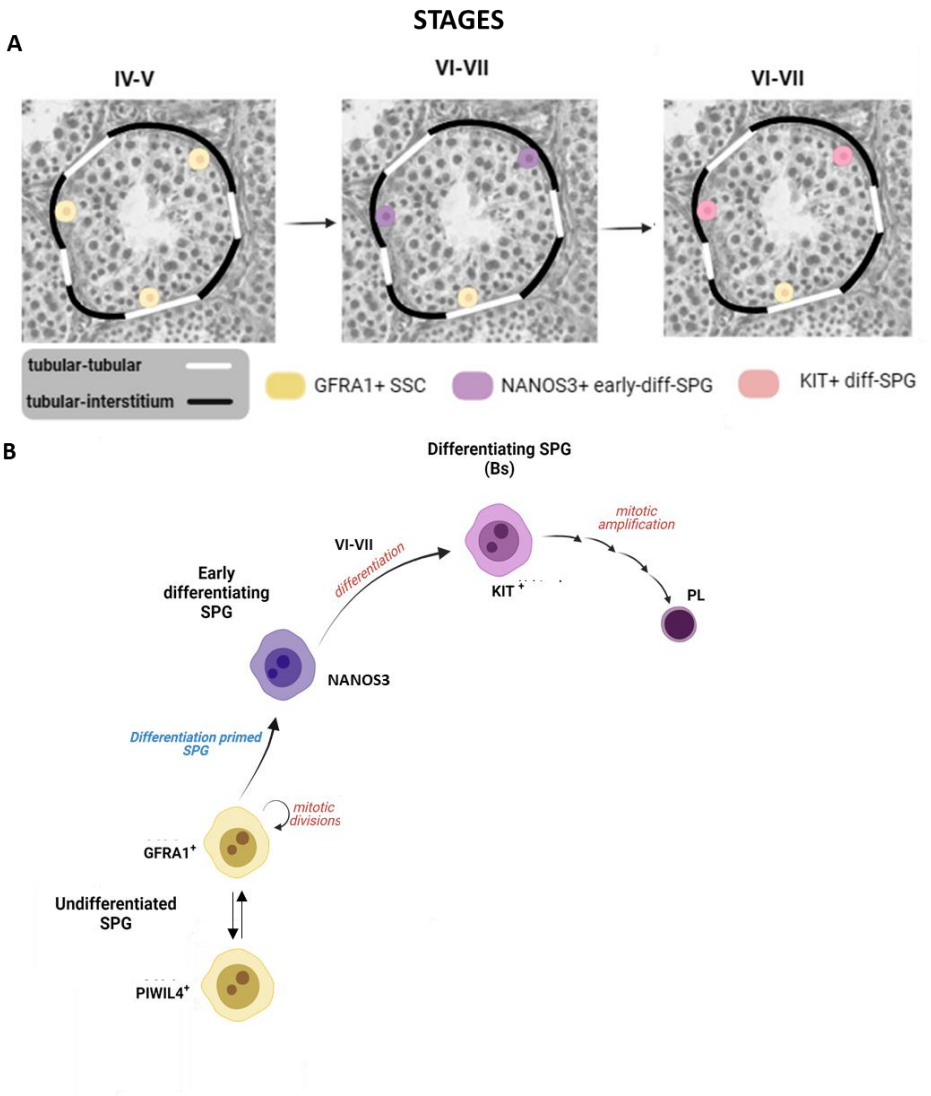

Figure 21: *A) A graphical abstract of the histological localization of undiff-SPG, early diff-SPG and diff-SPG along the basal lamina of seminiferous tubule. B) Tentative model for position-dependent spermatogonial progression in adult primates (modified from Capponi et al. 2023).*

Our study highlights the essential role of the histological analysis for the investigation of cell behaviour, differentiation, and interactions within their microenvironment. Because of the absence of animal model for lineage tracking or loss/gain of functions studies, experimental validation of this model is out of reach at current time. Nevertheless, the model may represent a starting point for future studies adding to the growing body of literature aimed at unravelling the complexities of SSC biology and spermatogenesis regulation in mammals. These findings have important implications for understanding male fertility, reproductive health, and the development of new SSC-targeted therapeutic interventions.

6. MATERIALS AND METHODS

6.1 Testicular biopsies

Monkey testicular tissue samples from cynomolgus monkey (*Macaca fascicularis*) were obtained from the institutional breading facility of University of Münster, Germany. Material from five mature animals was used for the study. Ethical approval for the use of cynomolgus monkey (license # 39.32.7.1) was obtained according to German federal law on the care and use of laboratory animals. Human testicular biopsies were used from heart-beating organ donors (n=3) at the hospital Policlinico Umberto I (Rome, Italy). For each donor, the free and informed consent of the family concerned, was obtained. The Ethical Committee of the hospital approved the use of human material according to national guidelines for organ donation as issued by the Italian Ministry of Public Health.

Monkey	Age	Sertoli cells /frame (150,0 x 150,0 µm)
#1	12 y	52
#2	9 y	63
#3	8 y	64
#4	8 y	61
#5	8 y	56
		60 mean of Sertoli cells/frame
Human samples	Age	
#1	42y	
#2	56y	

Table 1. *Table indicating all the samples used in this study. Age and Sertoli cells/frame for each monkey have been reported*

6.2 Immunofluorescence on FFPE

Immunofluorescence (IF) was performed as described previously (Grisanti et al., 2009). Formalin-fixed monkey and human testis samples were dehydrated with increasing concentrations of ethanol, embedded in paraffin, cut in 5 μm-thick sections, and mounted on polylysine-coated slides.

The sections were dewaxed and rehydrated. The antigen retrieval was performed incubating the slides in in citrate buffer pH 7.8 (UCS diagnostic, Morlupo, Italy) in a microwave oven at 750 W, three times for 5 minutes each.

In order to reduce the aldehyde-caused fluorescent background the sections were treated with Glycine 1M (Sigma-Aldrich, Milan, Italy) while the buffer with 1% bovine serum albumin (BSA) (Sigma-Aldrich, Milan, Italy) and 5% Normal Donkey Serum (Jackson Immuno Research Europe Ltd, Newmarket, UK) was used to avoid the unspecific antibody binding. The sections were incubated overnight at 4°C with the appropriate primary antibodies (Table 1). After the washes the sections were incubated with species specific secondary antibodies conjugated to ALEXA488 and Cy3 fluorochromes (Jackson Immuno Research Europe Ltd, Newmarket, UK) for 2 hours at room temperature. At the end the nuclei were counterstained with 4',6-diamidino-2-phenylindole, dihydrochloride (DAPI) (D1306 Thermo Fisher Scientific, Waltham, MA, 02451 USA). The slides were closed with Vectashield mounting medium (Vector Laboratories, Inc. Burlingame, CA, 94010 USA). The analysis was performed on photomicrographs acquired with a Zeiss Airy Scan 2 confocal microscope with 40x oil immersion objective.

6.3 Immunohistochemistry on FFPE

Immunohistochemistry (IHC) was performed as described previously (Grisanti et al., 2009). Bouin-fixed monkey and human testis samples were dehydrated with increasing concentrations of

ethanol, embedded in paraffin, cut in 5 μm-thick sections, and mounted on polylysine-coated slides.

The sections were dewaxed and rehydrated. The antigen retrieval was performed incubating the slides in citrate buffer pH 7.8 (UCS diagnostic, Morlupo, Italy) for the samples incubated with anti-BMP4, anti-BMPR1B, anti-PIWIL4, anti-GFRA1 or in citrate buffer pH 6.0 for the samples incubated with anti-NANOS3 and anti-KIT in a microwave oven at 750 W, three times for 5 minutes each.

For the immunohistochemistry after the antigen retrieval the quenching of endogenous peroxidase and the blocking of nonspecific binding with Super-Block (UltraTek HRP Anti-Polyvalent kit, ScyTek Laboratories) were performed on the sections. Sections were incubated overnight at 4°C with diluted primary antibody. After washing, sections were processed using the avidin-biotin peroxidase complex (ABC) procedure, according to the manufacturer's instructions (UltraTek HRP Anti-Polyvalent kit, ScyTek Laboratories). Negative control experiments were performed omitting the primary antibody. Peroxidase activity was revealed using 3,3'-diaminobenzidine-tetrahydrochloride (Roche Diagnostic, Monza, Italy), and nuclei were shortly counterstained with Mayer haematoxylin (PanReac AppliChem, ITW Reagents). After washing, for the samples incubated with anti-BMP4 and anti-BMPR1B sections were dehydrated through the ascending ethanol series, permanently mounted in Eukitt (Sigma). For the samples stained with anti-PIWIL4, anti-GFRA1, anti-NANOS3 and anti-cKIT, sections were further incubated 2h at room temperature with diluited 1:200 Lectin PNA conjugates (Molecular probes L-32458) for acrosomal detection and then closed with Vectashield mounting medium. The slides were analysed by light microscopy Zeiss, Axioskop 2 Plus.

6.4 Whole-mount immunofluorescence

Monkey and human seminiferous tubules were taken from testicular biopsies and immediately fixed in 4% PFA at 4°C for 4h. Fixed tubules were permeabilized with 0.5% Triton X100, treated with 1 M glycine for 1h, and with 0.1% TritonX-100, 1%BSA and 5% normal donkey serum in PBS overnight at 4°C. Next day, tubules were washed in Wash Buffer (1% BSA, 0.1% Triton X-100 in PBS) three times for 30 min and incubated overnight at 4°C with appropriate primary antibodies (Table 2). The following day, tubules were washed as above and incubated with species-specific secondary antibodies conjugated to Alexa 488-, Cy3- or Cy5-conjugated fluorochromes overnight at 4°C. Primary and secondary antibodies were diluted in 1% BSA and 0.1% Triton X-100 in PBS. After the secondary antibody, tubules were washed in Wash Buffer as above, and nuclei were stained with DAPI. Tubules were mounted onto slides using Vectashield mounting medium and observed using at Zeiss Airyscan 2 confocal microscope with 40× oil immersion objective. All images were taken under the same conditions. For each animal, at least 300 cells were randomly selected and analysed from several seminiferous tubules.

Antibody and Dilution	Species	Company (catalogue number)
BMPR1B (1:100)	Mouse	Abcam (ab78417)
BMP4 (1:50)	Rabbit	Abcam (ab124715)
RYK (1:100)	Rabbit	Proteintech (22138-1-AP)
WNT4A (1:50)	Mouse	Santa Crutz (sc-365370)
UCHL-1 (1:100)	Rabbit	Dako (Z5116)
PIWIL4 (1:100)	Rabbit	LifesSpan (LS-C482396)

GFRA1 (1:30)	Goat	R&D AF714
KIT (1:25)	Goat	R&D AF332
KI67 (1:100)	Rabbit	Abcam ab15580
NANOS3 (1:100)	Rabbit	Proteintech 21679-1-AP
ACROSIN (1:1000)	Mouse	Biosonda Biotechnology Acr-C5GF10
PNA (1:200)		Molecular Probes L-32458

Table 2. *Table indicating all the primary antibodies used in this study.*

6.5 Determination of the stages of the cycle of the seminiferous epithelium.

Stages identification in wholemounted tubules or testis sections, was based on the study of acrosomal development (using immunostaining for ACR or lectin PNA) and nuclear germ cell morphology using DAPI staining of elongating and elongated spermatids (Capponi et al., 2023; Di Persio et al., 2017; Muciaccia et al., 2013).

6.6 Imaging and quantification

In order to quantify the relative proportion of $BMPR1B^+$, $UCHL-1^+$, $PIWIL4^+$, $GFRA1^+$, KIT^+ and $KI67^+$ SPG in intact seminiferous tubules, at least three different testis samples were co-stained for relevant antibodies. The intensity of the staining was arbitrarily quantified as: +, week expression, ++, medium expression, +++ high expression. Due to the convoluted nature of monkey seminiferous tubules, in order to image the entire spermatogonial layer, z-stacks were acquired using Zeiss Airyscan 2 with a 40×oil immersion objective. For each staining analysis, 25-30 fields (150.0 x 150.0 μm) were randomly selected from at least six different seminiferous tubules for each animal. For each field of

analysis, confocal z-stacks were acquired (at 1 μm increments between z-slices). For each sample, at least 300 cells were randomly selected and analysed from several seminiferous tubules. All quantifications were performed using the ZEN BLUE edition. Quantitative data were normalized for 60 Sertoli cell nuclei. The number of Sertoli cell nuclei/field was quantified using SOX9 as marker (Table 1 shows the number of Sertoli cells/frame/ monkey).

6.7 Determining the position of spermatogonia in testicular parenchyma

For the study of the localization of spermatogonia in the testicular parenchyma was employed the method described by Chiarini-Garcia (Caldeira-Brant et al., 2020; Chiarini-Garcia et al., 2001; Chiarini-Garcia and Meistrich, 2008) Bouin's fixed 5mm-thick testis sections were stained with PIWIL4 or GFRA1 or NANOS3 or KIT followed by Lectin PNA and examined with the light microscope. Micrographs were taken with 10x objective from at least 25 microscopic fields for each sample, contained the selected cross sections. The same cross section was also acquired at 20X and 40X for detection of the stage or SPG subsets counts. All quantifications were performed on stored images using ImageJ.

For the Li calculation, two different colours were used to draw the perimeter of tubular cross sections on 10X images. A grey line was used to draw the portions of the tubule in which the peritubular tissue contacted other tubules; contact was defined as no visible space between the peritubular tissue of adjacent seminiferous tubules. A black line was used to draw the interface of the tubule peritubular tissue with the interstitial space. For each round tubule-cross section, the total length of each coloured line was calculated. Next, the number of $PIWIL4^+$ or $GFRA1^+$ or $NANOS3^+$ or KIT^+ spermatogonia were recorded as being opposite the interstitial or tubule contact areas in all the stages of the epithelial cycle for each animal.

The Strauss linear selectivity index (Li) was used to examine region selection by the different spermatogonial subsets in the

basal compartment of seminiferous tubules in each stage of the seminiferous epithelium (Strauss, 1979). In each staged round tubule- cross section, the Li was calculated for each tubule-tubule (t-t) and for tubule-interstitial region (t-i):

$$\mathbf{Li}_{(t-t)} = \mathbf{ri} - \mathbf{pi}$$

$$\mathbf{Li}_{(t-i)} = \mathbf{ri} - \mathbf{pi}$$

Li is the linear index value

ri is the proportion of the specific spermatogonial subset

pi is the proportion of length in the same region

These calculations resulted in an Li value for each region ranging from -1 to +1, with zero representing a random position of spermatogonia. Positive number (max 1) represented positive selection (preference) of the given region, while a negative number (max -1) represented negative selection (avoidance) of the specific region. In each animal, two Li values were obtained corresponding to tubule-interstitial area and tubule-tubule area for each of the twelve stages.

6.8 Statistical analysis

All quantitative data are shown as the mean±SEM. For the Li index analysis, to define the significance of the differences between many groups (i.e. the stages of the cycle), data were analysed using one-way analysis of variance (ANOVA) followed by Student-Newman-Keuls Method (All Pairwise Multiple Comparison Procedures between the pairs of stages). The significance level was fixed at P=0.05.

7. BIBLYOGRAPHY

Amann, R.P. (2008). The cycle of the seminiferous epithelium in humans: a need to revisit? Journal of andrology *29*, 469-487.

Aponte, P.M., van Bragt, M.P., de Rooij, D.G., and van Pelt, A.M. (2005). Spermatogonial stem cells: characteristics and experimental possibilities. APMIS : acta pathologica, microbiologica, et immunologica Scandinavica *113*, 727-742.

Bernstein, I.R., Nixon, B., Lyons, J.M., Damyanova, K.B., De Oliveira, C.S., Mabotuwana, N.S., Stanger, S.J., Kaiko, G.E., Ying, T.H., Oatley, J.M., *et al.* (2023). The hypoxia-inducible factor EPAS1 is required for spermatogonial stem cell function in regenerative conditions. iScience *26*, 108424.

Boitani, C., Di Persio, S., Esposito, V., and Vicini, E. (2016). Spermatogonial cells: mouse, monkey and man comparison. Seminars in cell & developmental biology *59*, 79-88.

Brinster, R.L., and Avarbock, M.R. (1994). Germline transmission of donor haplotype following spermatogonial transplantation. Proceedings of the National Academy of Sciences of the United States of America *91*, 11303-11307.

Buaas, F.W., Kirsh, A.L., Sharma, M., McLean, D.J., Morris, J.L., Griswold, M.D., de Rooij, D.G., and Braun, R.E. (2004). Plzf is required in adult male germ cells for stem cell self-renewal. Nature genetics *36*, 647-652.

Bush, S.J., Nikola, R., Han, S., Suzuki, S., Yoshida, S., Simons, B.D., and Goriely, A. (2024). Adult Human, but Not Rodent, Spermatogonial Stem Cells Retain States with a Foetal-like Signature. Cells *13*.

Caldeira-Brant, A.L., Martinelli, L.M., Marques, M.M., Reis, A.B., Martello, R., Almeida, F., and Chiarini-Garcia, H. (2020). A subpopulation of human Adark spermatogonia behaves as the reserve stem cell. Reproduction (Cambridge, England) *159*, 437-451.

Capponi, C., Palazzoli, M., Di Persio, S., Fera, S., Spadetta, G., Franco, G., Wistuba, J., Schlatt, S., Neuhaus, N., de Rooij, D., *et al.* (2023). Interplay of spermatogonial subpopulations during initial stages of spermatogenesis in adult primates. Development (Cambridge, England) *150*.

Capponi, C., & Vicini, E. (2023). The Biology of Male Reproduction and Infertility Current Understanding of the Physiology and Histology of Human Spermatogenesis. *Men's Reproductive and Sexual Health Throughout the Lifespan: An Integrated Approach to Fertility, Sexual Function, and Vitality*, 23.

Carlomagno, G., van Bragt, M.P., Korver, C.M., Repping, S., de Rooij, D.G., and van Pelt, A.M. (2010). BMP4-induced differentiation of a rat spermatogonial stem cell line causes changes in its cell adhesion properties. Biology of reproduction *83*, 742-749.

Chan, F., Oatley, M.J., Kaucher, A.V., Yang, Q.E., Bieberich, C.J., Shashikant, C.S., and Oatley, J.M. (2014). Functional and molecular features of the Id4+ germline stem cell population in mouse testes. Genes & development *28*, 1351-1362.

Chiarini-Garcia, H., Hornick, J.R., Griswold, M.D., and Russell, L.D. (2001). Distribution of type A spermatogonia in the mouse is not random. Biology of reproduction *65*, 1179-1185.

Chiarini-Garcia, H., and Meistrich, M.L. (2008). High-resolution light microscopic characterization of spermatogonia. Methods in molecular biology (Clifton, NJ) *450*, 95-107.

Ciller, I., Palanisamy, S., Ciller, U., Al-Ali, I., Coumans, J., and McFarlane, J. (2023). Steroidogenic enzyme gene expression and testosterone production are developmentally modulated by bone morphogenetic protein receptor-1B in mouse testis. Physiological research *72*, 359-369.

Clermont, Y. (1966a). Renewal of spermatogonia in man. The American journal of anatomy *118*, 509-524.

Clermont, Y. (1966b). Spermatogenesis in man. A study of the spermatogonial population. Fertility and sterility *17*, 705-721.

Clermont, Y. (1969). Two classes of spermatogonial stem cells in the monkey (Cercopithecus aethiops). The American journal of anatomy *126*, 57-71.

Clermont, Y., and Antar, M. (1973). Duration of the cycle of the seminiferous epithelium and the spermatogonial renewal in the monkey Macaca arctoides. The American journal of anatomy *136*, 153-165.

Clermont, Y., Leblond, C.P., and Messier, B. (1959). [Duration of the cycle of the seminal epithelium of the rat]. Archives d'anatomie microscopique et de morphologie experimentale *48(Suppl)*, 37-55.

Costoya, J.A., Hobbs, R.M., Barna, M., Cattoretti, G., Manova, K., Sukhwani, M., Orwig, K.E., Wolgemuth, D.J., and Pandolfi, P.P. (2004). Essential role of Plzf in maintenance of spermatogonial stem cells. Nature genetics *36*, 653-659.

Davidoff, M.S., Middendorff, R., Koeva, Y., Pusch, W., Jezek, D., and Müller, D. (2001). Glial cell line-derived neurotrophic factor (GDNF) and its receptors GFRalpha-1 and GFRalpha-2 in the human testis. Italian journal of anatomy and embryology = Archivio italiano di anatomia ed embriologia *106*, 173-180.

de Kretser, D.M., Loveland, K.L., Meehan, T., O'Bryan, M.K., Phillips, D.J., and Wreford, N.G. (2001). Inhibins, activins and follistatin: actions on the testis. Molecular and cellular endocrinology *180*, 87-92.

de Rooij, D.G., and Russell, L.D. (2000). All you wanted to know about spermatogonia but were afraid to ask. Journal of andrology *21*, 776-798.

DeFalco, T., Potter, S.J., Williams, A.V., Waller, B., Kan, M.J., and Capel, B. (2015). Macrophages Contribute to the Spermatogonial Niche in the Adult Testis. Cell reports *12*, 1107-1119.

Di Persio, S., and Neuhaus, N. (2023). Human spermatogonial stem cells and their niche in male (in)fertility: novel concepts from single-cell RNA-sequencing. Human reproduction (Oxford, England) *38*, 1-13.

Di Persio, S., Saracino, R., Fera, S., Muciaccia, B., Esposito, V., Boitani, C., Berloco, B.P., Nudo, F., Spadetta, G., Stefanini, M., *et al.* (2017). Spermatogonial kinetics in humans. Development *144*, 3430-3439.

Di Persio, S., Tekath, T., Siebert-Kuss, L.M., Cremers, J.F., Wistuba, J., Li, X., Meyer Zu Hörste, G., Drexler, H.C.A., Wyrwoll, M.J., Tüttelmann, F., *et al.* (2021). Single-cell RNA-seq unravels alterations of the human spermatogonial stem cell

compartment in patients with impaired spermatogenesis. Cell reports Medicine *2*, 100395.

Ehmcke, J., Luetjens, C.M., and Schlatt, S. (2005). Clonal organization of proliferating spermatogonial stem cells in adult males of two species of non-human primates, Macaca mulatta and Callithrix jacchus. Biology of reproduction *72*, 293-300.

Endo, T., Freinkman, E., de Rooij, D.G., and Page, D.C. (2017). Periodic production of retinoic acid by meiotic and somatic cells coordinates four transitions in mouse spermatogenesis. Proceedings of the National Academy of Sciences of the United States of America *114*, E10132-e10141.

Endo, T., Romer, K.A., Anderson, E.L., Baltus, A.E., de Rooij, D.G., and Page, D.C. (2015). Periodic retinoic acid-STRA8 signaling intersects with periodic germ-cell competencies to regulate spermatogenesis. Proceedings of the National Academy of Sciences of the United States of America *112*, E2347-2356.

Fietz, D., and Bergmann, M. (2017). Functional Anatomy and Histology of the Testis. In Endocrinology of the Testis and Male Reproduction, M. Simoni, and I. Huhtaniemi, eds. (Cham: Springer International Publishing), pp. 1-29.

Fouquet, J.P., and Dadoune, J.P. (1986). Renewal of spermatogonia in the monkey (Macaca fascicularis). Biology of reproduction *35*, 199-207.

Gassei, K., and Orwig, K.E. (2013). SALL4 expression in gonocytes and spermatogonial clones of postnatal mouse testes. PloS one *8*, e53976.

Golden, J.P., DeMaro, J.A., Osborne, P.A., Milbrandt, J., and Johnson, E.M., Jr. (1999). Expression of neurturin, GDNF, and GDNF family-receptor mRNA in the developing and mature mouse. Experimental neurology *158*, 504-528.

Grasso, M., Fuso, A., Dovere, L., de Rooij, D.G., Stefanini, M., Boitani, C., and Vicini, E. (2012). Distribution of GFRA1-expressing spermatogonia in adult mouse testis. Reproduction (Cambridge, England) *143*, 325-332.

Grisanti, L., Falciatori, I., Grasso, M., Dovere, L., Fera, S., Muciaccia, B., Fuso, A., Berno, V., Boitani, C., Stefanini, M., *et al.* (2009). Identification of spermatogonial stem cell subsets by morphological analysis and prospective isolation. Stem cells (Dayton, Ohio) *27*, 3043-3052.

Guo, J., Grow, E.J., Mlcochova, H., Maher, G.J., Lindskog, C., Nie, X., Guo, Y., Takei, Y., Yun, J., Cai, L., *et al.* (2018). The adult human testis transcriptional cell atlas. Cell research *28*, 1141-1157.

Hara, K., Nakagawa, T., Enomoto, H., Suzuki, M., Yamamoto, M., Simons, B.D., and Yoshida, S. (2014). Mouse spermatogenic stem cells continually interconvert between equipotent singly isolated and syncytial states. Cell stem cell *14*, 658-672.

Heller, C.G., and Clermont, Y. (1963). Spermatogenesis in man: an estimate of its duration. Science (New York, NY) *140*, 184-186.

Heller, C.H., and Clermont, Y. (1964). KINETICS OF THE GERMINAL EPITHELIUM IN MAN. Recent progress in hormone research *20*, 545-575.

Hermann, B.P., Cheng, K., Singh, A., Roa-De La Cruz, L., Mutoji, K.N., Chen, I.C., Gildersleeve, H., Lehle, J.D., Mayo, M.,

Westernströer, B., *et al.* (2018). The Mammalian Spermatogenesis Single-Cell Transcriptome, from Spermatogonial Stem Cells to Spermatids. Cell reports *25*, 1650-1667.e1658.

Hermann, B.P., Sukhwani, M., Hansel, M.C., and Orwig, K.E. (2010). Spermatogonial stem cells in higher primates: are there differences from those in rodents? Reproduction (Cambridge, England) *139*, 479-493.

Hermann, B.P., Sukhwani, M., Simorangkir, D.R., Chu, T., Plant, T.M., and Orwig, K.E. (2009). Molecular dissection of the male germ cell lineage identifies putative spermatogonial stem cells in rhesus macaques. Human reproduction (Oxford, England) *24*, 1704-1716.

Hess, R.A., and Renato de Franca, L. (2008). Spermatogenesis and cycle of the seminiferous epithelium. Advances in experimental medicine and biology *636*, 1-15.

Hu, J., Chen, Y.X., Wang, D., Qi, X., Li, T.G., Hao, J., Mishina, Y., Garbers, D.L., and Zhao, G.Q. (2004). Developmental expression and function of Bmp4 in spermatogenesis and in maintaining epididymal integrity. Developmental biology *276*, 158-171.

Huckins, C., and Oakberg, E.F. (1978). Morphological and quantitative analysis of spermatogonia in mouse testes using whole mounted seminiferous tubules. II. The irradiated testes. The Anatomical record *192*, 529-542.

Inoue, H., Sakurai, T., Hasegawa, K., Suzuki, A., and Saga, Y. (2022). NANOS3 suppresses premature spermatogonial differentiation to expand progenitors and fine-tunes spermatogenesis in mice. Biology open *11*.

Khanehzad, M., Abbaszadeh, R., Holakuyee, M., Modarressi, M.H., and Nourashrafeddin, S.M. (2021). FSH regulates RA signaling to commit spermatogonia into differentiation pathway and meiosis. Reproductive biology and endocrinology : RB&E *19*, 4.

Kitadate, Y., Jörg, D.J., Tokue, M., Maruyama, A., Ichikawa, R., Tsuchiya, S., Segi-Nishida, E., Nakagawa, T., Uchida, A., Kimura-Yoshida, C., *et al.* (2019). Competition for Mitogens Regulates Spermatogenic Stem Cell Homeostasis in an Open Niche. Cell stem cell *24*, 79-92.e76.

Kossack, N., Terwort, N., Wistuba, J., Ehmcke, J., Schlatt, S., Schöler, H., Kliesch, S., and Gromoll, J. (2013). A combined approach facilitates the reliable detection of human spermatogonia in vitro. Human reproduction (Oxford, England) *28*, 3012-3025.

Koubova, J., Menke, D.B., Zhou, Q., Capel, B., Griswold, M.D., and Page, D.C. (2006). Retinoic acid regulates sex-specific timing of meiotic initiation in mice. Proceedings of the National Academy of Sciences of the United States of America *103*, 2474-2479.

Lau, X., Munusamy, P., Ng, M.J., and Sangrithi, M. (2020). Single-Cell RNA Sequencing of the Cynomolgus Macaque Testis Reveals Conserved Transcriptional Profiles during Mammalian Spermatogenesis. Developmental cell *54*, 548-566.e547.

Li, X., Fang, Y., Chen, L., Quan, H., Wang, Y., and Ge, R.S. (2022). Bone morphogenetic protein 4 inhibits rat stem/progenitor Leydig cell development and regeneration via SMAD-dependent and SMAD-independent signaling. Cell death & disease *13*, 1039.

Lord, T., and Nixon, B. (2020). Metabolic Changes Accompanying Spermatogonial Stem Cell Differentiation. Developmental cell *52*, 399-411.

Mäkelä, J.A., and Hobbs, R.M. (2019). Molecular regulation of spermatogonial stem cell renewal and differentiation. Reproduction (Cambridge, England) *158*, R169-r187.

Meng, X., Lindahl, M., Hyvonen, M.E., Parvinen, M., de Rooij, D.G., Hess, M.W., Raatikainen-Ahokas, A., Sainio, K., Rauvala, H., Lakso, M., *et al.* (2000). Regulation of cell fate decision of undifferentiated spermatogonia by GDNF. Science *287*, 1489-1493.

Morales, A., and Cavicchia, J.C. (2002). Spermatogenesis and blood-testis barrier in rats after long-term Vitamin A deprivation. Tissue & cell *34*, 349-355.

Morrison, S.J., and Spradling, A.C. (2008). Stem cells and niches: mechanisms that promote stem cell maintenance throughout life. Cell *132*, 598-611.

Muciaccia, B., Boitani, C., Berloco, B.P., Nudo, F., Spadetta, G., Stefanini, M., de Rooij, D.G., and Vicini, E. (2013). Novel stage classification of human spermatogenesis based on acrosome development. Biology of reproduction *89*, 60.

Nakagawa, T., Jörg, D.J., Watanabe, H., Mizuno, S., Han, S., Ikeda, T., Omatsu, Y., Nishimura, K., Fujita, M., Takahashi, S., *et al.* (2021). A multistate stem cell dynamics maintains homeostasis in mouse spermatogenesis. Cell reports *37*, 109875.

Nakagawa, T., Nabeshima, Y., and Yoshida, S. (2007). Functional identification of the actual and potential stem cell compartments in mouse spermatogenesis. Developmental cell *12*, 195-206.

Nakagawa, T., Sharma, M., Nabeshima, Y., Braun, R.E., and Yoshida, S. (2010). Functional hierarchy and reversibility within the murine spermatogenic stem cell compartment. Science (New York, NY) *328*, 62-67.

Nakamura, Y., Jörg, D.J., Kon, Y., Simons, B.D., and Yoshida, S. (2021). Transient suppression of transplanted spermatogonial stem cell differentiation restores fertility in mice. Cell stem cell *28*, 1443-1456.e1447.

Nicholls, P.K., Harrison, C.A., Rainczuk, K.E., Wayne Vogl, A., and Stanton, P.G. (2013). Retinoic acid promotes Sertoli cell differentiation and antagonises activin-induced proliferation. Molecular and cellular endocrinology *377*, 33-43.

Oakberg, E.F. (1956). A description of spermiogenesis in the mouse and its use in analysis of the cycle of the seminiferous epithelium and germ cell renewal. The American journal of anatomy *99*, 391-413.

Oatley, J.M., Avarbock, M.R., and Brinster, R.L. (2007). Glial cell line-derived neurotrophic factor regulation of genes essential for self-renewal of mouse spermatogonial stem cells is dependent on Src family kinase signaling. The Journal of biological chemistry *282*, 25842-25851.

Oatley, J.M., and Brinster, R.L. (2008). Regulation of spermatogonial stem cell self-renewal in mammals. Annual review of cell and developmental biology *24*, 263-286.

Pellegrini, M., Grimaldi, P., Rossi, P., Geremia, R., and Dolci, S. (2003). Developmental expression of BMP4/ALK3/SMAD5 signaling pathway in the mouse testis: a potential role of BMP4 in

spermatogonia differentiation. Journal of cell science *116*, 3363-3372.

Plant, T.M. (2010). Undifferentiated primate spermatogonia and their endocrine control. Trends in endocrinology and metabolism: TEM *21*, 488-495.

Puglisi, R., Montanari, M., Chiarella, P., Stefanini, M., and Boitani, C. (2004). Regulatory role of BMP2 and BMP7 in spermatogonia and Sertoli cell proliferation in the immature mouse. European journal of endocrinology *151*, 511-520.

Ramaswamy, S., Razack, B.S., Roslund, R.M., Suzuki, H., Marshall, G.R., Rajkovic, A., and Plant, T.M. (2014). Spermatogonial SOHLH1 nucleocytoplasmic shuttling associates with initiation of spermatogenesis in the rhesus monkey (Macaca mulatta). Molecular human reproduction *20*, 350-357.

Saracino, R., Capponi, C., Di Persio, S., Boitani, C., Masciarelli, S., Fazi, F., Fera, S., and Vicini, E. (2020). Regulation of Gdnf expression by retinoic acid in Sertoli cells. Molecular reproduction and development *87*, 419-429.

Schmierer, B., and Hill, C.S. (2007). TGFbeta-SMAD signal transduction: molecular specificity and functional flexibility. Nature reviews Molecular cell biology *8*, 970-982.

Scholzen, T., and Gerdes, J. (2000). The Ki-67 protein: from the known and the unknown. Journal of cellular physiology *182*, 311-322.

Schwarzer, J.U., Fiedler, K., v Hertwig, I., Krüsmann, G., Würfel, W., Schleyer, M., Mühlen, B., Pickl, U., and Löchner-Ernst, D. (2003). Sperm retrieval procedures and intracytoplasmatic

spermatozoa injection with epididymal and testicular sperms. Urologia internationalis *70*, 119-123.

Shami, A.N., Zheng, X., Munyoki, S.K., Ma, Q., Manske, G.L., Green, C.D., Sukhwani, M., Orwig, K.E., Li, J.Z., and Hammoud, S.S. (2020). Single-Cell RNA Sequencing of Human, Macaque, and Mouse Testes Uncovers Conserved and Divergent Features of Mammalian Spermatogenesis. Developmental cell *54*, 529-547.e512.

Sharma, M., and Braun, R.E. (2018). Cyclical expression of GDNF is required for spermatogonial stem cell homeostasis. Development (Cambridge, England) *145*.

Simorangkir, D.R., Marshall, G.R., Ehmcke, J., Schlatt, S., and Plant, T.M. (2005). Prepubertal expansion of dark and pale type A spermatogonia in the rhesus monkey (Macaca mulatta) results from proliferation during infantile and juvenile development in a relatively gonadotropin independent manner. Biology of reproduction *73*, 1109-1115.

Simorangkir, D.R., Marshall, G.R., and Plant, T.M. (2009). A re-examination of proliferation and differentiation of type A spermatogonia in the adult rhesus monkey (Macaca mulatta). Human reproduction (Oxford, England) *24*, 1596-1604.

Sohni, A., Tan, K., Song, H.W., Burow, D., de Rooij, D.G., Laurent, L., Hsieh, T.C., Rabah, R., Hammoud, S.S., Vicini, E., *et al.* (2019). The Neonatal and Adult Human Testis Defined at the Single-Cell Level. Cell reports *26*, 1501-1517.e1504.

Stine, R.R., and Matunis, E.L. (2013). Stem cell competition: finding balance in the niche. Trends in cell biology *23*, 357-364.

Strauss RE 1-7-1979 Reliability Estimates for Ivlev's Electivity Index, the Forage Ratio, and a Proposed Linear Index of Food Selection. *Transactions of the American Fisheries Society* 108 344-352.

Sugimoto, R., Nabeshima, Y., and Yoshida, S. (2012). Retinoic acid metabolism links the periodical differentiation of germ cells with the cycle of Sertoli cells in mouse seminiferous epithelium. Mechanisms of development *128*, 610-624.

Suzuki, H., Sada, A., Yoshida, S., and Saga, Y. (2009). The heterogeneity of spermatogonia is revealed by their topology and expression of marker proteins including the germ cell-specific proteins Nanos2 and Nanos3. Developmental biology *336*, 222-231.

Tokunaga, Y., Imai, S., Torii, R., and Maeda, T. (1999). Cytoplasmic liberation of protein gene product 9.5 during the seasonal regulation of spermatogenesis in the monkey (Macaca fuscata). Endocrinology *140*, 1875-1883.

Trupp, M., Rydén, M., Jörnvall, H., Funakoshi, H., Timmusk, T., Arenas, E., and Ibáñez, C.F. (1995). Peripheral expression and biological activities of GDNF, a new neurotrophic factor for avian and mammalian peripheral neurons. The Journal of cell biology *130*, 137-148.

Unni, S.K., Modi, D.N., Pathak, S.G., Dhabalia, J.V., and Bhartiya, D. (2009). Stage-specific localization and expression of c-kit in the adult human testis. The journal of histochemistry and cytochemistry : official journal of the Histochemistry Society *57*, 861-869.

van Alphen, M.M., van de Kant, H.J., and de Rooij, D.G. (1988). Depletion of the spermatogonia from the seminiferous epithelium

of the rhesus monkey after X irradiation. Radiation research *113*, 473-486.

van Pelt, A.M., and de Rooij, D.G. (1991). Retinoic acid is able to reinitiate spermatogenesis in vitamin A-deficient rats and high replicate doses support the full development of spermatogenic cells. Endocrinology *128*, 697-704.

Vernet, N., Dennefeld, C., Klopfenstein, M., Ruiz, A., Bok, D., Ghyselinck, N.B., and Mark, M. (2008). Retinoid X receptor beta (RXRB) expression in Sertoli cells controls cholesterol homeostasis and spermiation. Reproduction (Cambridge, England) *136*, 619-626.

Voog, J., and Jones, D.L. (2010). Stem cells and the niche: a dynamic duo. Cell stem cell *6*, 103-115.

Yoshida, S. (2010). Stem cells in mammalian spermatogenesis. Development, growth & differentiation *52*, 311-317.

Yoshida, S. (2018). Open niche regulation of mouse spermatogenic stem cells. Development, growth & differentiation *60*, 542-552.

Yoshida, S. (2020). Mouse Spermatogenesis Reflects the Unity and Diversity of Tissue Stem Cell Niche Systems. Cold Spring Harbor perspectives in biology *12*.

Yoshida, S., Sukeno, M., and Nabeshima, Y. (2007). A vasculature-associated niche for undifferentiated spermatogonia in the mouse testis. Science (New York, NY) *317*, 1722-1726.

Yoshinaga, K., Nishikawa, S., Ogawa, M., Hayashi, S., Kunisada, T., Fujimoto, T., and Nishikawa, S. (1991). Role of c-kit in mouse spermatogenesis: identification of spermatogonia as a specific site

of c-kit expression and function. Development (Cambridge, England) *113*, 689-699.

Zhao, G.Q., Deng, K., Labosky, P.A., Liaw, L., and Hogan, B.L. (1996). The gene encoding bone morphogenetic protein 8B is required for the initiation and maintenance of spermatogenesis in the mouse. Genes & development *10*, 1657-1669.

Zheng, K., Wu, X., Kaestner, K.H., and Wang, P.J. (2009). The pluripotency factor LIN28 marks undifferentiated spermatogonia in mouse. BMC developmental biology *9*, 38.

Zirkin, B.R., and Papadopoulos, V. (2018). Leydig cells: formation, function, and regulation. Biology of reproduction *99*, 101-111.

8. LIST OF PUBLICATIONS

Capponi C, **Palazzoli M**, Di Persio S, Fera S, Spadetta G, Franco G, Wistuba J, Schlatt S, Neuhaus N, de Rooij D, Vicini E. Interplay of spermatogonial subpopulations during initial stages of spermatogenesis in adult primates. Development. 2023 15;150(10):dev201430. doi: 10.1242/dev.201430.

Conferences

Capponi Chiara; **Palazzoli, Martina**; Di Persio Sara; Fera Stefania; Wistuba Joachim; Schlatt, Stefan; Neuhaus Nina &Vicini, Elena. Distribution of the spermatogonial subpopulations during the stages of the epithelial cycle and their relative position along the basal membrane. European Testis Workshop 18-21 June 2023, Montreux, Switzerland. (Communication selected for oral presentation).

Palazzoli, Martina; Capponi, Chiara; Di Persio Sara; Fera Stefania; Wistuba Joachim; Schlatt, Stefan; Neuhaus Nina &Vicini, Elena. Distribution of the spermatogonial subpopulations during the stages of the epithelial cycle and their relative position along the basal membrane of the seminiferous tubules. Scientific Session, Assemblea del Collegio Docenti di Istologia ed Embriologia february 2024, Rome, Italy. (Communication selected for oral presentation).

Palazzoli, Martina; Capponi, Chiara; Di Persio Sara; Fera Stefania; Wistuba Joachim; Schlatt, Stefan; Neuhaus Nina &Vicini, Elena. Distribution of the spermatogonial subpopulations during the stages of the epithelial cycle. 16th Meeting of the Network of Young Researchers in Andrology 27-29 May 2024, Bruxelles, Belgium. (Communication selected for oral presentation).

Palazzoli, Martina; Capponi, Chiara; Di Persio Sara; Fera Stefania; Wistuba Joachim; Schlatt, Stefan; Neuhaus Nina &Vicini, Elena. Distribution of the spermatogonial subpopulations during the stages of the epithelial cycle. XI BeMM Symposium 30 september, Rome, Italy.

9. ATTACHMENT

Report on training, research and other activities carried out in the last year of PhD

My Ph.D. project is focused on the analysis of primate's spermatogonial compartment regulation, by validating possible niche-derived signaling molecules and by analyzing the topological distribution of different spermatogonial subpopulations along the basal membrane of the seminiferous tubules.

Specifically, in the third year of my Ph.D., I analyzed the distribution of the diff-SPG along the basal lamina of the seminiferous tubules during the seminiferous epithelial cycle.

I started the characterization of the early diff-SPG testing the expression of NANOS3, a promising marker, conserved both in human and non-human primate, recently proposed by scRNAseq analysis to characterize early stages of spermatogonial differentiation. I found that a major part of the $NANOS3^{+}$ SPG preferentially resides in the tubular regions facing the interstitium at stages VI-VII. Continuing the analysis for the first generation of diff-SPG (B1), also in this case we discovered a preference of the KIT^{+}SPG for the tubular regions adjacent to the interstitium at stages VI-VII of the seminiferous epithelial cycle.

Finally, I propose a scheme for position-related spermatogonial progression in primates. The results of my thesis have been included in Miniposter titled "Distribution of the spermatogonial subpopulations during the stages of the epithelial cycle and their relative position along the basal membrane" presented at European Testis Workshop. My Miniposter has been selected for plenary oral presentation. In the last two months I have been working at my PhD dissertation.

During the last year of Ph.D. I have been involved in didactical activity, specifically I supported my supervisor Prof. Elena Vicini

in the execution of online exams of the course “Histology and Embryology” for medical students. Moreover, I have participated in various training initiatives, as well as congresses, courses and seminars as listed below.

Conferences

22st European Testis Workshop, 18-21 June 2023, Montreux, Switzerland. (Communication selected for oral presentation).

Seduta Scientifica, Assemblea del Collegio Docenti di Istologia ed Embriologia. february 2024, Rome, Italy.

16th Meeting of the Network of Young Researchers in Andrology 27-29 May 2024, Bruxelles, Belgium. (Communication selected for oral presentation).

XI BeMM Symposium 30 september, Rome, Italy.

Courses

9 -16/05/24 Preparing artwork for scientific papers – 4th edition.

Seminars

- 16/11/2023 “The power of flow-cytometry” Dott.ssa Giovanna Borsellino
- 21/11/2023 “Building biomimetic nanomaterials to interact with the biology of the body” Prof. Ennio Tasciotti
- 14/12/2023 “Medical AI: historical and bioethical background (I)” Prof. Andrea Grignolio
- 18/01/2024 “Medical AI: historical and bioethical background (II)” Prof. Andrea Grignolio
- 14/02/2024 “Toxicity of denatured protein aggregates and neurodegenerative diseases” Prof. Fabrizio Chiti

- 15/02/2024 “Epigenetic and transcriptional alterations in male germ cells dysfunction” Dott. Sara Di Persio

- 29/02/2024 “Effects of altered gravitational force on human male germ cell lines: omics approaches" PhD student Alessia Di Pauli: “Bioprinted BloodBrain Barrier Model for Evaluating Efficacy of Lipid Nanoparticles in Brain Cancer Treatment" PhD Student Ginevra Friggeri

- 14/03/2024 “Investigating the therapeutic role and molecular regulation of the oncomiR miR444and miR-4488 in drug resistant melanomas" PhD student Arianna Ortolano; “AntiSense Oligonucleotides (ASO) based treatment in Amyotrophic Lateral Sclerosis" PhD student Martina Lupoli

- 21/03/2024 “Role of Schwann cells-cancer cells crosstalk in Hepatocellular carcinoma progression" PhD student Elisa Pizzichini;"Plasmonic Biosensor for Real-Time Detection and Quantification of DNA Released from Stimuli Responsive Nano Delivery Systems" PhD student Maria Laura Sforza; "Development of a delivery system to target KRAS mutations in Ductal Pancreatic Adenocarcinoma in vivo" PhD student Abbinantefina Annalisa Pia

- 26/03/2024 Symposium: The attractiveness of a scientific career in the third millennium

- 04/04/2024 "HDAC4 functions in mediating the crosstalk between skeletal muscle and fibro-adipogenic progenitors in Duchenne Muscular Dystrophy" PhD student Giorgi Cavioli; "Comparison of denoising techniques in ultra-high field fMRI data and their effect on different brain tissues" PhD student Giovanni Giulietti

- 11/04/2024 "X-MET: a bioengineered muscle construct as a model to study muscle physiopathology" PhD student Mariam Zouhair

- 18/04/2024 " **β** -Sarcoglycanopathy (LGMDR4): a study of muscle diversity using a Sgc**β** KO mouse model" PhD student Michela Gloriani

- 30/04/2024 "Inflammaging: inflammation in the old age" Prof. Marcello Pinti

- 09/05/2024 “The representation of the hand in the resting human brain" PhD student Cristina Perciballi; “Detection of micro- and nano- plastics and the assessment of their potential health risks" PhD student Siyao Xiao

- 16/05/2024 "3D culture systems for evaluating Microgravity effects on the male gonad" PhD student Marika Berardini

- 20/05/2024 "Ageing-related degenerative processes in models derived from patients with accelerated ageing" Prof. Miria Ricchetti

- 23/05/2024 “Characterization of molecular players promoting functional remodelling in the ex vivo muscle engineered tissue (X-MET)” PhD student Desiree Genovese; “Removing barriers to DNA replication in terminally differentiated cells” PhD student Gladio Giannitelli

- 30/05/2024 “Characterization of the AML bone marrow microenvironment response to Azacitidine +Venetoclax treatment" PhD student Gilla Mazzanti; “Custom-engineered extracellular vesicles to counteract muscle degenerations" PhD student Martina Biglietto

- 27/06/2024 “Plasmonic nanostructures for optical and thermoplasmonic-based healthcare applications" PhD student Federica Zaccagnini; “Role of Epigenetic and Metabolic Reprogramming in Normal and Neoplastic Hematopoiesis" PhD student Alessandra Zaza

10. ANSWERS TO THE REVIEWERS

Reviewer 1

This thesis is very well written and the work is presented clearly. Overall I congratulate the student for a job well done. I have only minor suggestions that would improve the presentation of the data and the text. Moreover, I have a few corrections of typos and mistakes.

Suggestions:

1. It is not clear how or why exactly the two ligand-receptor pairs were selected for further evaluation. The explanation sounds very vague.
I better motivated the choice of the two ligand-receptor pairs on the result section (paragraph 4.1.1).
2. I would remove, as much as possible, abbreviations from the section titles.
Done as requested
3. Some references are very old. I have nothing against old references but in some cases new information exists it is advisable to add that in addition to or instead the old reference. I advise the student to go through the text and identify where a more recent reference would be useful.
Done as suggested
4. page 5, line 6 - I believe “domain” is the wrong word here.
In the revised Thesis, the sentence: “has a wider expression domain” has been changed to: “broader expression pattern”.
5. Page 7, line 2-4 - this sentence is rather reductive, as spermatogenesis (and this thesis shows it very well) is influenced by more than Sertoli cells. I suggest rewriting.
Done as suggested.
6. Page 7, last sentence before Figure 1 - there are cells missing between PL spermatocytes and spermatids. Please complete.

I thank the reviewer for pointing out this point. Amended as suggested.

7. page 9, page 12, there is no need to define spermatogenesis multiple times. Please edit.

Done as suggested.

8. Page 10 - I think it is important to refer that the organisation of the seminiferous epithelium cycles into stages is ultimately a artificial and spermatogenesis is very much a continuum and not static as it might seem at first sight. So much so that the cycle and cell types have been continuously refined, as is referred later on in the introduction.

I agree with the reviewer. I rephrase the sentence on page 10.

9. It is important to specifically define what is meant by "monkey" in this thesis. For example, in the legend of figure 3 it is unclear to what species monkey refers to. This is true throughout the text. I suggest very clearly stating "In this thesis, monkey refers to species …" early in the text.

I added the information about the species of monkey in the legend to Fig.3. The species of monkey used in all the experiments were stated early in the text (i.e. the summary, aims etc.).

10. page 13, lines 10-11 - Inhibin B is not exclusively a product of Sertoli cells. It is a compound product of Sertoli and germ cells, which is why the levels are high in individuals with full spermatogenesis and very low in SCO. Only when there are germ cells is there sufficient Inhibin B to cause a negative feedback on FSH.

I performed an extensive search, but I could not find references showing that Inhibin B is produced by germ cells.

11. The expression "primitive" spermatogonia is sometimes used but I do not think this is the correct way of putting it. The word primitive seems to indicate a much earlier cell type than the one I believe is meant here. Perhaps early spermatogonia would be a better option.

Done as suggested.

12. Page 27- the first sentence of the second paragraph is confusing and it is not immediately clear why this subpopulation is so interesting.
Done as suggested
13. Some figures are split between several pages. It would be preferable to simply make several figures. For example figures 11 and 12 suffer from this problem, however in my opinion there is an easy way to solve this that makes it easier for the reader to look at the data. The IF figures for both human and monkey should be together in one figure, which will make it easier to compare the patterns. The tables should not be split between human and monkey but joined, again to make it easier to compare the species.
I thank the reviewer for these useful suggestions. I modified the figures as suggested.
14. Generally for IF and IHC it would be good to point out in the micrographs examples of the cells that are highlighted in the text.
Done as suggested
15. Figure 13 - negative controls are missing.
Done as suggested
16. Page 40 - the last two sentences are very confusing and should be edited for clarity.
Done as suggested.
17. Page 49, line 6 from the bottom and page 51, line 3 of the main text: I assume by cross-section you mean round tubule/tubular cross section? Please clarify here and wherever relevant.
Done as suggested.
18. page 60, first paragraph - I don't think the data is enough to suggest that the position regulates the proliferation, more likely you can hypothesize that this is the case.
I changed this line as follows: "these data suggest" into "we speculate that".
I also wonder whether the analysis has enough statistical power to determine the association of cells with localisation. What is the effect of chance and of histological artefacts on the findings?

We have established our sample size based on similar papers reporting the non-random distribution of spermatogonia in rodents (Chiarini-Garcia et al., 2001; Chiarini-Garcia et al., 2003)
To ensure the robustness of our findings, we analyzed multiple tissue sections from different testis regions to account for potential artifacts caused by sectioning or staining variability in all the animals analyzed (n=3). Furthermore, in our analysis only well-preserved regions including round tubular-cross sections were included in the final dataset.

19. page 70, statistical analysis - are parametric statistics the right way to evaluate these data? Moreover, where/why were Tuckey or Kruskal-Wallis tests used?

For the data on the Li index, normality of the data was confirmed using the Shapiro-Wilk test ($p > 0.05$), and variances were found to be homogenous using Equal Variance Test (Brown-Forsythe) ($p > 0.05$). Therefore, parametric statistics were applied. Please note that, the post-hoc test employed was ***Student-Newman-Keuls (SNK) method not*** *the Tuckey or Kruskal-Wallis methods, as erroneously indicated in the first version of the thesis.*

Typos and mistakes for correction:

I correct all the highlighted typos and errors like suggested

Reviewer 2

The work does not yet reach the quality for publication. I doubt that the data are sufficient to write two papers.
Strengths: The findings confirm already published data and add (a bit of) new information to the field.
Weaknesses: only one technique was applied in this PhD project; data are limited; data are difficult to interpret due to suboptimal data analysis; the discussion lacks important aspects (limitations, implications, future perspectives).

General comments

-Numbering of (sub)titles should be double-checked, as well as the alignment in the index
Done as suggested
-Language editing is recommended (typo's, grammatical errors, use of Italian words)
Done as suggested
-The use of abbreviations should be double-checked: full (abbrev) at 1st mentioning, afterwards only the abbrev.
Done as suggested
-Use subscript for spg types: e.g. Ap, B1
In this study I'm using specific markers for the two broad classes of spg types (undifferentiated and differentiating spermatogonia). These markers cannot discriminate for Ap, Ad, B (Di Persio et al., 2017; Capponi et al., 2023).
-Write Latin species names in italic
Done as suggested
-Several paragraphs in the introduction start with more or less the same sentence. Try to explain the events in a (chrono)logical way.
The introduction has been modified as suggested.
-How sure are you about the staining and the identification of the different cell types? Without the use of cell-specific markers, this is very difficult to interpret
The identification of different spg is based on established markers (UCHL1, PIWIL4, GFRA1, KIT), the stage of the cycle and their nuclear morphology (*Di Persio, 2017; Capponi, 2023).*
-The discussion lacks limitations of the current study, implications for research (and clinic) and future perspectives.
I add this informations in the discussion as requested
Other comments
-P9: the fig is not in line with the text on p7 (cfr. spc in adlum comp)
We have aligned the text and fig. 2.

-P35: penultimate sentence needs a reference or show the results
Done as suggested.
-How did you quantify the cells in fig 11 and 12?
As specified in the Material and method section, I did not quantify the percentage of positive cells.
What corresponds to +, ++ and +++? For example, in fig 12B/D, very few LCs are stained for BMP4, but the score is +++. This is confusing.
The + symbols correspond to an arbitrary estimation of fluorescence intensity. I added this information to the Material and method section.
-Fig 13 shows a lot of background staining. Please add negative controls.
Done as requested
-Fig14: expressing % cells per frame is not the best way to show the results. It would be better to show the % of BMPR1B positive cells amongst the UCHL1+ ones or amongst the entire spg pool (same for the other markers).
We have modified Fig14, the % of positive cells are expressed per 100 Sertoli (Capponi et al., 2023).
A major concern here is how spg will be identified. Purely on morphology? How many of the cells in the frame are not spg? What cells are these?
Imagining has been done on the basal layer of the tubules, that contains all the spermatogonia and some primary spermatocytes as previously shown (Corallini,2006; Grisanti, 2009; Grasso, 2012; Dovere, 2013; Di Persio, 2017; Capponi, 2023). The identification of different spg is based on established markers (UCHL1, PIWIL4, GFRA1, KIT) and/or nuclear morphology to distinguish them from unlabeled germ cells.
The numbers shown in the text seem to differ from the graphs (eg. BMPR1B+/UCHL1- cells in B does not seem to be 8%). Do you mention the mean in the text? I would recommend showing the data as mean+SD or median (ranges), depending on the graphs and statistics to be used (parametric vs non-parametric tests). If

showing means, SD is preferred over SEM as SEM shows technical errors and SD shows biological variation.
Data were expressed as median (ranges). In the text, I modified the numbers from mean to median values. I added more details on box plots description in the legends.
-Fig 16: how did you determine the stages in this exp?
In wholemounts staining the stage was determined using the co-staining with acrosin as detailed in Material and method section. I added this information also in the result section (page 46).
-Fig 17/18: numbers are expressed per cross-section. Were only round cross-sections included? If not, this could have biased your results.
Yes, only round tubule-cross sections were included.
Add the stages that are shown on the pictures.
Done as suggested.
How was the total number of spg determined?
For data reported in 17D, a total of 25 round tubule-cross sections were evaluated for a total number of 192 PIWIL4$^+$ spg.
Show exact p-values in case there is statistical difference.
Done as suggested
In C, the total should be 100%, not 1.
Done as requested.
-Fig 20: the stainings and pictures are not optimal. The pictures are difficult to interpret as the staining is not much different from the background.
I replace the representative staining with a better picture.
-P58: "BMPR1B is expressed in all the undiff-SPG": I don't think you can state this, as in fig 14B, some UCHL1+ cells were negative for BMPR1B. Same for p60 "BMPR1B is a general marker for the undifferentiated SPG".
We reformulate our statements as follows: BMPR1B is expressed in almost all the undiff-SPG.
-P62: what's new in the scheme compared to already published data (fig 10)?

In the novel version I propose that the early differentiating spg expresses NANOS3.

-P66: last sentence: 300 cells were selected: based on what? (also on p68)

The cells were randomly selected in the tubular round-cross sections employed for LI index analysis.

-Table 1: please add categorie numbers

Done as requested.

-P67: which marker did you use to identify stages?

As stated in paragraph 6.5 we used acrosin staining or lectin PNA-568 .

-P68: first sentence: add reference or scheme

We added the references as requested.

-Add the ages of the monkeys/humans to the Methods section. If there would be a large variety amongst the individuals, ages should also be mentioned in the figure legends.

I added a new Table including the age of monkeys/humans.